

DESIGN AND CALIBRATION OF A THERMAL SYPHON HEAT TRANSFER
LOOP UTILIZING FREON 12 NEAR THE CRITICAL STATE

By

EUGENE CHARLES NESTLE

u

Bachelor of Science

Oklahoma State University

Stillwater, Oklahoma

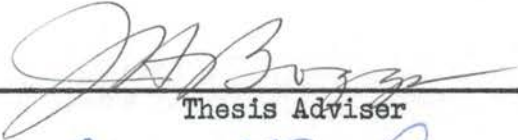
1957

Submitted to the faculty of the Graduate School of
the Oklahoma State University
in partial fulfillment of the requirements
for the degree of
MASTER OF SCIENCE
August 1958


NOV 7 1958

DESIGN AND CALIBRATION OF A THERMAL SYPHON HEAT TRANSFER
LOOP UTILIZING FREON 12 NEAR THE CRITICAL STATE


Thesis Approved:



Thesis Adviser



Carroll M. Leonard



Dean of the Graduate School

410275

ACKNOWLEDGEMENT

It is fitting to take this opportunity to recognize and to thank those who helped make this thesis possible.

Mention should first of all be made of the General Electric Company whose grant made possible the partial sponsorship of this research.

The counsel and assistance of Dr. James H. Boggs throughout the entire M. S. program is greatly appreciated by the writer, and indebtedness is acknowledged to Professor C. M. Leonard who reviewed the thesis.

The splendid work of Laboratory Supervisor, Professor Bert S. Davenport and technicians, John A. McCandless and George Cooper in assisting and advising with the construction of the thermal syphon bears recognition.

The writer is indebted to Dr. Jack P. Holman, whom he assisted with construction of the apparatus and accompanying research. The association with Dr. Holman, together with his advice, continued encouragement, and humor proved priceless in value to the writer and his contributions are gratefully acknowledged.

Most important of all, the writer wishes to thank his own mother and father whose encouragement, sacrifices, and perseverance throughout his academic career are appreciated more than they can ever realize. Truly, had it not been for them, the past several years would not have been so enjoyable nor so richly rewarding. To them and to those mentioned above go a sincere and heartfelt "thank you."

TABLE OF CONTENTS

Chapter	Page
I. INTRODUCTION	1
II. PREVIOUS INVESTIGATIONS	4
III. THEORY OF THE THERMAL SYPHON	9
IV. DESIGN OF THE THERMAL SYPHON	15
Heat Transfer Loop	15
Test Section and Heating Element	18
Power Supply	20
Heat Exchanger and Flow Control	20
Instrumentation Facilities	26
V. OPERATING CONSIDERATIONS	38
VI. CALIBRATION OF EQUIPMENT	44
Venturi Calibration	44
Thermocouple Calibrations	50
Calibration of Temperature Recorder	56
VII. SUMMARY AND CONCLUSIONS	60
SELECTED BIBLIOGRAPHY	63
APPENDIXES	65

LIST OF TABLES

Table	Page
I. National Bureau of Standards Freezing Point Samples	50
II. Thermocouple Calibration Equations	57
III. Physical Dimensions of the Loop	66
IV. Physical Properties of Type 304 Stainless Steel Tubing . .	69

LIST OF PLATES

Plate	Page
I. Rear View of Test Apparatus	18
II. Test Panel	27
III. Panel and Instrument Wiring	30
IV. Vacuum Apparatus	42

LIST OF FIGURES

Figure	Page
1. Schematic of Thermal Syphon	10
2. Schematic Diagram of the Thermal Syphon Heat Transfer Loop.	16
3. Test Section Details	20
4. Test Panel Wiring Diagram.	22
5. Heat Exchanger Schematic	24
6. Instrument Wiring Diagram	28
7. Line Cooler and Thermocouple Well Details	32
8. Venturi Meter	33
9. Thermocouple Measuring Circuit	36
10. Venturi Calibration Setup	46
11. Venturi Calibration Curve	49
12. Thermocouple Calibration Circuit and Furnace	52
13. Bulk Thermocouple Calibration Curve	54
14. Wall Thermocouple Calibration Curve	55
15. Temperature Recorder Calibration Curve	58
16. Thermal Conductivity of AISI Type 304 Stainless Steel . . .	70
17. Electricial Resistivity of AISI Type 304 Stainless Steel. .	71
18. Solutions of Kreith-Summerfield Equation	74

CHAPTER I

INTRODUCTION

The ever increasing demands of science and industry in the production of power have exerted great influence in the realm of heat transfer. Any process which involves the generation of heat has associated with it the problems of obtaining suitable means of transferring this thermal energy. The ability of a system to transfer heat is dependent, in part, on the size of the heat transfer surface available so that a desired rate of transfer could be prohibited by space limitations. If a system could be devised so that its working mechanism would promote high heat transfer rates with a minimum of surface area, the problems concerned with space limitations would be largely overcome.

Many heat exchange devices operate on the principle of heat convection, a heat transfer process in which thermal energy is exchanged between moving parts of a fluid or between these and surfaces of different temperature. This process is described by Newton's equation as

$$q = h A \Delta t, \quad \text{I-1}$$

in which q = heat transfer, Btu per hr;

h = a factor of proportionality known as a film coefficient of heat transfer, Btu per hr ft² °F;

A = surface perpendicular to direction of heat flow, ft²;

Δt = temperature difference between the area, A , of a surface and the fluid in contact with it, °F.

Because of the preceding equation, it is seen that if a system could be developed such that its influence on the film coefficient would cause it to increase in magnitude, high rates of heat transfer would be possible without a corresponding large increase in area. An increase in film coefficient is dependent on the characteristics of a specific fluid. It is expected that the film coefficient will reach its maximum value at the critical point where the enthalpy of vaporization of a fluid is equal to zero.

If a method of correlation could be developed such that the behavior of the film coefficient under different operating conditions of a system could be predicted, it would be possible to design similar systems for given heat transfer requirements.

A natural circulation experimental loop with an electrically heated tube or test section was designed and built in the Mechanical Engineering Laboratories of Oklahoma State University for the purpose of investigating the feasibility of such an apparatus and for the purpose of investigating the heat transfer characteristics of Freon 12 in the critical region. The device shall be called a thermal syphon heat transfer loop.

The object of this thesis was to design the thermal syphon apparatus which has proved quite satisfactory in preliminary investigations of Freon 12 in the vicinity of the critical point. Freon 12, dichlorodifluoromethane, was chosen for the test fluid because its low critical temperature and pressure permitted a relatively simple design. Descriptions of the auxiliary equipment used in conjunction with the thermal syphon are also given together with suggested methods of control and operation of the various components of the system. Finally, a description of the methods used to calibrate the equipment is presented

together with the calibration curves for the equipment.

One may vision the practical use of a workable thermal syphon in the cooling of a nuclear reactor in which one of the problems of heat removal is the obtaining of high heat fluxes in confined spaces. The circulating fluid of the thermal syphon would receive heat from the reactor in place of the electrically heated test section and, for a large system, could conceivably transfer this heat to a steam generator.

CHAPTER II

PREVIOUS INVESTIGATIONS

Heat transfer loops are rapidly becoming quite prominent in experimental research since many designs and types have been built which depend on the application and type of study being carried on. Descriptions of several previously built experimental heat transfer loops are presented in this chapter in order that some of the design considerations may be emphasized and compared with the apparatus described in this thesis.

A report by Wissler, Isbin, and Amundson (1) on the transient operation of a natural-circulation loop presented the design of a heat transfer loop built for the purpose of studying the oscillatory behavior of the temperatures and flow rates of the circulating fluid.

This particular loop, using water as the circulating fluid, was constructed primarily of 16-gage, 1-in. O. D. hard drawn brass tubing. The loop contained a 216-in. vertical pressure-drop test section.

The heater consisted of four 7.5 kw Chromalox immersion heaters, and a horizontal concentric tube heat exchanger was used to cool the fluid. A heater and pump were installed to regulate the temperature and flow rate of the cooling water. The volumetric flow rate of the circulating fluid was measured by an electromagnetic flow meter. The valving was so arranged that forced circulation could be employed by use of a pump and rotameters. Surge tanks using compressed air were used to regulate the pressure and reduce pressure fluctuations.

Dickinson and Welch (2) determined heat transfer coefficients for supercritical water flowing in an electrically heated stainless steel tube having an inside diameter of 0.300-in. Bulk fluid temperatures were varied from 220 to 1000°F at pressures of 4500 and 3500 psi. The mass flow rate was varied from 1.6 to 2.5 x 10⁶ lb per hr ft² and heat flux from 280,000 to 580,000 Btu per hr ft².

The circulating water was preheated before entering the test section in a small once-through single-tube steam generator making it possible to control fluid temperatures between 210 and 1000°F. at the test section inlet by varying the boiler firing rate. The test section outlet pressure was controlled by throttling.

The flow was controlled by a feed pump and flow rate was measured by a calibrated nozzle. A mixed-bed deionizer was added to the system to keep contaminants to a minimum.

Power was supplied to the test section from three 40 kva transformers connected with secondary taps in series and regulated by an automatic control that maintained a constant heat input to the test section.

Kaufman and Henderson (3) obtained forced-convection heat transfer data for water flowing in a 0.689-in. electrically heated Inconel tube at pressures up to 2000 psi and temperatures in the non-boiling region. The water velocities ranged from 5 to 35 feet per second and the flow rate was regulated by controlling the pump speed, and by a valve in the by-pass around the pump.

A unique pressurizing system was employed in this particular loop. The test section was enclosed in a stainless steel casing which acted as a supercharge housing for the test section. The system was pressurized by nitrogen supplied from storage cylinders through a regulator valve to

the accumulator and test section casing. System pressures up to 2000 psi were used to obtain a balance of pressure between the circulating fluid and the supercharging gas in the test section casing.

Kaufman and Isely (4) conducted further research on heat transfer film coefficients using a loop containing a 10 1/4-in. length of 0.204-in. I. D. electrically heated Inconel tubing. Arrangements were made for pre-heating the circulating water by addition of a steam heater to the loop. To facilitate accurate fluid temperature measurements, calming and mixing tanks were installed in the system. The circulating water flowed into the calming tank before entering the test section and through a mixing tank after leaving the section. The calming and mixing tanks were made of three concentric cylinders so arranged that the water made three axial passes upon entering and leaving the test section. A honeycomb in the calming tank straightened the flow of water entering the heater tube and a set of baffles in the mixing tank ensured thorough mixing of the water leaving the test section.

A 0.01-in. diameter platinum wire was used by Doughty and Drake (5) to determine free-convection heat transfer coefficients for a horizontal circular cylinder using Freon 12 as the test fluid. The wire was mounted inside an 8-in. diameter steel pipe test chamber so arranged to allow charging with a test fluid, and variation of the charge, pressure, and temperature. The platinum test cylinder was supported at the midpoint of the steel pipe by two 14 gage copper wires. These copper wires were covered with porcelain insulators around which were wound Nichrome resistance wire for guard-heating purposes. These guard heaters were thermally insulated from the test gas by mica tubing packed with Sauereisen cement.

The test vessel was heated by passing an electric current through Teflon insulated Nichrome heating wires wound over the surface of the vessel in such a way as to obtain a uniform surface temperature.

The weight of the charge in the system was measured by supporting the test vessel on a platform scale.

Test-cylinder end temperatures were indicated by chromel-alumel thermocouples silver soldered to each end of the platinum wire and the voltage drop across the cylinder was measured by using these attached thermocouples as potential leads. The temperature of the test fluid was indicated by four thermocouples inserted at varying lengths into the fluid through the bottom of the test vessel.

Schmidt, Eckert, and Grigull (6) investigated the heat transfer characteristics of ammonia in a thermal syphon type apparatus similar to the one under present consideration. The loop consisted of a closed circulatory oval shaped system made of stainless steel pipe with 0.5907-in. inside diameter.

The test section was heated by passing an electric current through a nichrome strip that was wound around the pipe over thin nicanite. A cooling jacket was brazed onto the pipe and divided in the middle perpendicularly to the pipe axis by a rubber sleeve to absorb uneven thermal expansions of the jacket.

Cooling was accomplished either by using tap water or glycol flowing through a Hoppler thermostat. The pressure fluctuations in the water pipe were eliminated by the use of an overflow.

The test pipe was charged through an intermediate tank which was supported on a platform scale so the weight of the charge could be determined.

No method for measuring the flow rate of the circulating fluid was provided. Tube wall temperatures were measured by manganin-constantan thermocouples soldered to the outside of the pipe, above and below the heat exchanger, but no provisions were made for determining test section tube wall temperatures.

CHAPTER III

THEORY OF THE THERMAL SYPHON

Heat transfer in a thermal syphon loop occurs by convection due to fluid motion in which fluid adjacent to a hot surface receives heat which it imparts to the bulk of the fluid by mixing.

The heat transfer process peculiar to the thermal syphon system may be described by referring to the basic types of convection heat transfer; free convection, and forced convection.

In free or natural convection, the convective currents in a system are caused by density differences brought about by temperature gradients. The cause of the fluid motion is a net buoyant force existing between two adjacent regions of the fluid. This force is a result of the differential thermal expansion caused by the temperature difference associated with the flow of heat.

The fluid flow due to forced convection is produced by the pressure differential induced in the system by mechanical apparatus. This flow rate is not usually dependent on temperature gradients or heat flux.

In the thermal syphon loop diagrammed in Figure 1, a temperature gradient and thus a density gradient exists in the system as a result of the heating in the test section and subsequent cooling in the heat exchanger. As a result of the density differences, a pressure differential is also present throughout the system. This pressure differential, and thus the flow rate, is dependent on the heat flux.

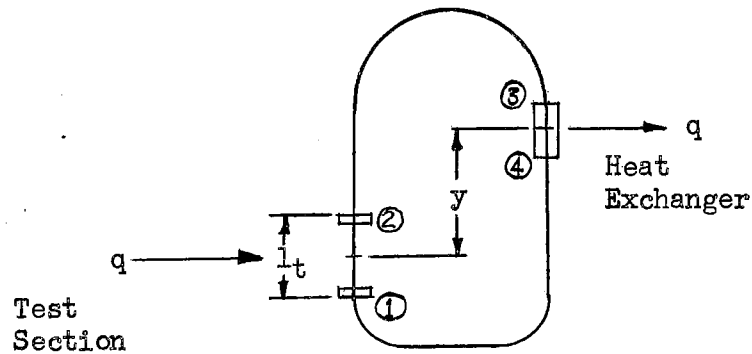


Fig. 1. Schematic of Thermal Syphon.

It is seen that convection heat transfer in a thermal syphon cannot be described simply as a free convection process in which transfer of heat is brought about solely by a thermal lifting force or by forced convection in which the flow rate and heat flux are independent variables. Instead, heat transfer in a thermal syphon is similar in some respects to both of these two basic types of convection heat transfer.

According to the theories developed by Schmidt, Eckert, and Grigull (6), the flow rate of the fluid caused by the addition and removal of equal amounts of heat, q , is developed in such a way that the thermal lifting force is completely balanced by frictional forces so that flow equilibrium is achieved.

The pressure differential caused by the thermal lifting forces may be expressed as:

$$\Delta p = y \delta_m \beta_m \Delta t_p, \quad \text{III-1}$$

where, Δp = pressure differential, lb per ft²;

y = vertical distance between center of test section and
center of heat exchanger, ft;

δ_m = mean specific weight of the fluid, evaluated at the arithmetic mean bulk temperature in the loop, lb per ft³;
 β_m = mean volume coefficient of expansion evaluated at the arithmetic mean bulk temperature, °F⁻¹; and
 Δt_b = fluid bulk temperature difference = $t_{2b} - t_{1b} = t_{3b} - t_{4b}$, °F.

In order to overcome the pipe friction of the loop, the lifting force, for laminar flow, must be equal to:

$$\Delta p = \frac{64 \mu u l}{d_i^2}, \quad \text{III-2}$$

where, μ = dynamic viscosity evaluated at the arithmetic mean bulk temperature, lb sec per ft²;
 u = mean fluid velocity, ft per sec;
 l = one half the length of the loop measured along the pipe axis, ft; and
 d_i = inside pipe diameter, ft.

For turbulent flow in smooth pipes, the frictional resistance is expressed by the Blasius Law:

$$\Delta p = 0.316 \text{Re}^{-\frac{1}{4}} \delta_m \frac{u^2 l}{g d}, \quad \text{III-3}$$

where, Re = Reynolds number = $\left(\frac{\delta u d}{\mu g} \right)$; and
 g = gravitational constant, ft per sec².

The heat absorbed by the fluid is equal to the product of the weight rate of flow, specific heat at constant pressure, and temperature difference. It may be expressed as:

$$q = \omega c_p \Delta t_b = \delta_m A_i u c_p \Delta t_b, \quad \text{III-4}$$

where, q = total heat added in the test section, Btu per hr;
 ω = weight rate of fluid flow, lb per hr;
 c_p = specific heat at constant pressure, Btu per lb °F; and
 A_1 = inside cross sectional area of the tube, ft².

In an effort to predict heat transfer phenomena, Schmidt, Eckert, and Grigull defined an apparent heat conductivity, k_a , which may be expressed by the equation:

$$q = k_a A_1 \frac{\Delta t_b}{l} \quad \text{III-5}$$

It was then possible to establish a relationship between apparent heat conductivity coefficient and the true heat conductivity coefficient, k , by obtaining suitable ratios of the coefficients which are characteristic of laminar or turbulent flow of the fluid.

By combining Equations (1), (2), (4), and (5), the ratio of apparent heat conductivity to true heat conductivity for the laminar case may be expressed as:

$$\frac{k_s}{k} = \frac{y \delta_m^2 \beta_m \Delta t_b d_i^2 c_p}{64 \mu k}, \quad \text{III-6}$$

or

$$\frac{k_s}{k} = \frac{1}{64} \text{Gr Pr}(y/d), \quad \text{III-7}$$

where, $\text{Gr} = \text{Grashof number}, \frac{6 \Delta t d^3 \gamma^2}{g \mu^2}$; and

$\text{Pr} = \text{Prandtl number}, \frac{c_p \mu}{k}$.

An equivalent expression for the turbulent case for smooth pipe may be formulated using Equation (3) in place of Equation (2) such that:

$$\frac{k_s}{k} = \text{Pr Gr}^{4/7} (1/d) (y/l)^{4/7} 0.316^{-4/7} \quad \text{III-8}$$

Equations (7) and (8) give an indication of the expected increase in the rate of heat transfer at the critical point. Since the specific heat for constant pressure and the thermal coefficient of expansion increase to very large values in the critical region, the presence of these terms in Equations (7) and (8) indicates an increase in heat transfer.

Holman (7) extended the work of Schmidt, Eckert, and Grigull, and obtained an expression for the film coefficient of heat transfer. This film coefficient may be defined as:

$$h = \frac{q}{A_d \Delta t_f} \quad \text{III-9}$$

where, $A_d = \pi d_i l_t$, ft^2 ;

l_t = length of test section tube, ft; and

Δt_f = film temperature difference, $^{\circ}\text{F}$.

The resulting correlations may be expressed as:

$$\text{Nu} = 16 (\text{Re})^2 (\text{Pr}) (\text{Gr}_f)^{-1} (1/l_t) (d/y) \quad \text{III-10}$$

for the laminar case; and

$$\text{Nu} = 0.079 (\text{Re})^{11/4} (\text{Pr}) (\text{Gr}_f)^{-1} (1/l_t) (d/y), \quad \text{III-11}$$

for the turbulent case,

where, $\text{Nu} = \text{Nusselt number} = \frac{h d}{k}$.

The dimensional constants of the loop are:

$$l = 109.3 \text{ in.}$$

$$l_t = 25.25 \text{ in.}$$

$$d_i = 0.430 \text{ in.}$$

$$y = 37.0 \text{ in.}$$

By inserting these numerical constants, Equation (10) is reduced to:

$$\frac{\text{Nu Gr}_f}{\text{Pr}} = 0.805 \text{ Re}^2, \quad \text{III-12}$$

and Equation (11) becomes:

$$\frac{\text{Nu Gr}_f}{\text{Pr}} = 0.00397 \text{ Re}^{11/4} \quad \text{III-13}$$

Subsequent experimentation (7) verified the validity of Equation (13) with reasonable accuracy and the fact that this correlation differs from the conventional forced convection expression:

$$\text{Nu} = 0.023 \text{ Re}^{0.8} \text{ Pr}^{0.4} .$$

CHAPTER IV

DESIGN OF THE THERMAL SYPHON

The principal components of the thermal syphon system are: (1) heat transfer loop proper, (2) test section and heating element, (3) power supply, (4) heat exchanger and flow control, and (5) instrumentation facilities. Figure 2 shows the relative location of these components in the loop. Each component will be described separately.

Heat Transfer Loop

The heat transfer loop is an elongated oval in design measuring 93-in. in height and 218.6-in. around the axial perimeter. Constructed of AISI Type 304 Stainless Steel Tubing of 0.500-in. O.D. and 0.430-in. I.D., the loop has a cubic capacity of 31.74 cubic inches. As shown in Fig. 2, the top of the loop forms a semi-circular arc while the bottom contains a straight section for inclusion of the venturi meter. These smooth, large radii provide direction change of the flow with as little disturbance to the fluid as possible. The curved sections were formed by bending the tubing around plywood forms in which a system of rollers was used.

Stainless steel, because of its high corrosion resistance, enables high temperature operations without contamination of the fluid. The smooth interior surface of the tube promotes even and positive flow of the circulating fluid without danger of the formation of excessive

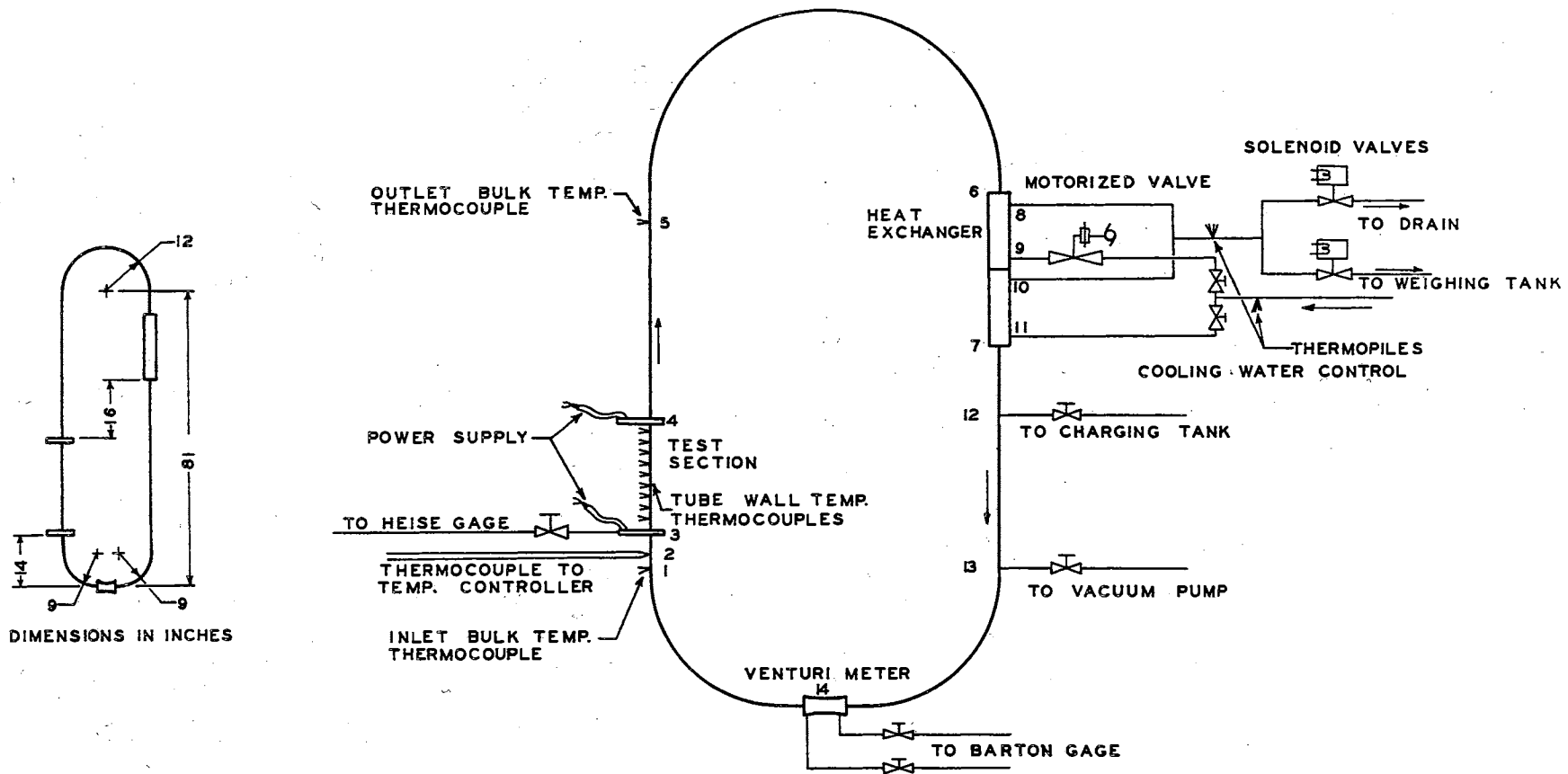


Fig. 2. Schematic Diagram of the Thermal Syphon Heat Transfer Loop.

scale or sludge.

Appendix B contains a list of the physical properties of stainless steel; and also, a graphical representation of the variation of the thermal conductivity and electrical resistivity with temperature.

All connections in the loop were made by the use of Swagelok stainless steel fittings. Since the flexibility of the oval was sufficient to equalize the uneven thermal expansions of the tubing, expansion joints were unnecessary. A suitable sealant was found in the use of Swagelok's "Blue Goop", an effective anti-seize compound for use with stainless steel. This compound retained its sealant properties at the elevated temperatures employed in the system.

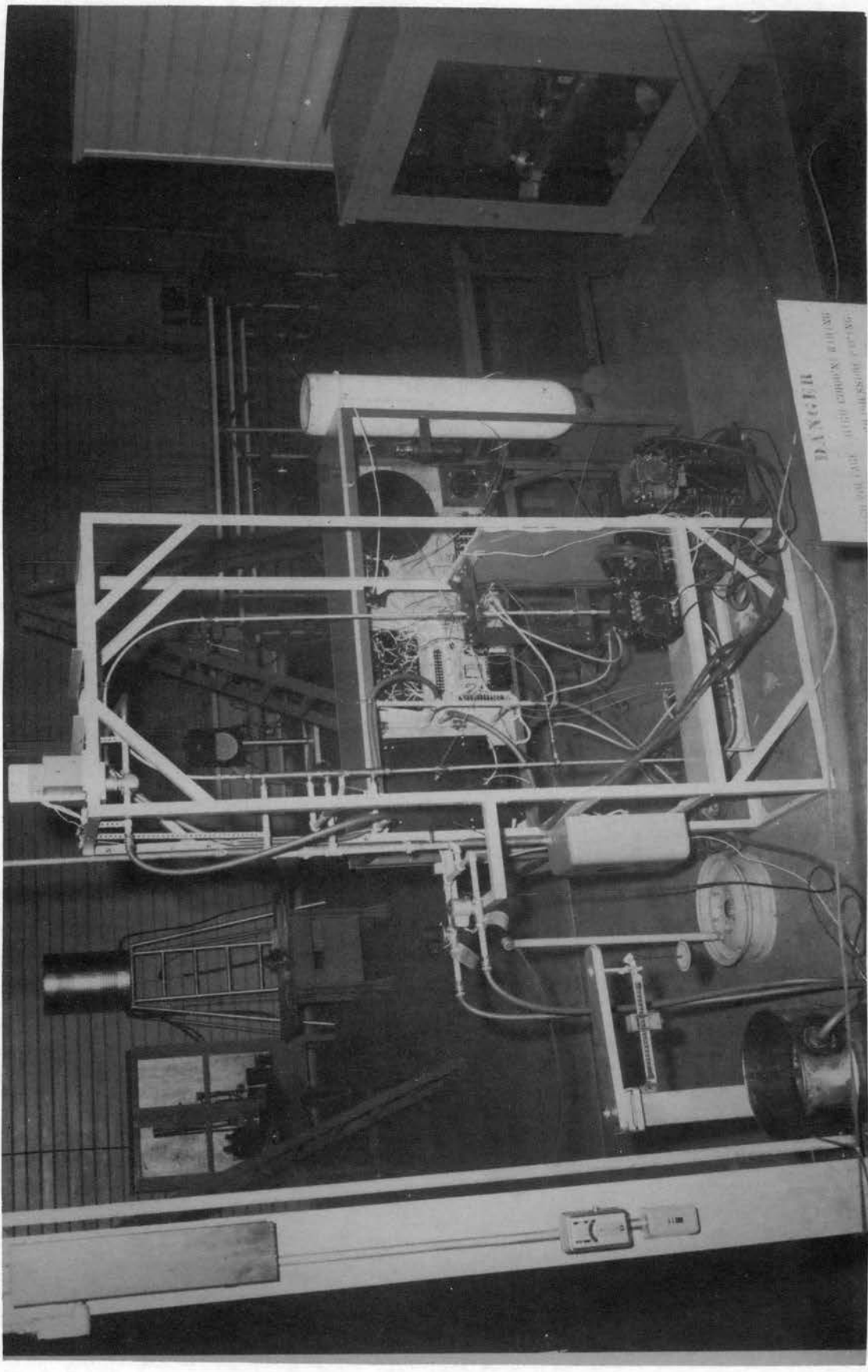
Because of the materials used in the construction of the thermal syphon and the subsequent methods of assembly and sealing, it was possible to obtain maximum operating temperature and pressure in the system of approximately 700°F and 1000 psi, respectively.

The assembled loop was supported inside a framework constructed of 1 1/2-in. angle iron. Plate I shows the thermal syphon loop as it is positioned within the framework. Rigid support was provided by steel strapping at the top and sides of the loop and by bolting the test section flanges to the frame.

The fluid used in the thermal syphon loop was Freon 12, dichlorodifluoromethane. This commercial refrigerant, a product of the E. I. du Pont de Nemours Company, is a high purity compound having the following specifications as listed by the manufacturer:

Maximum water content, ppm by wt.	10
Maximum non-absorbable gas,	
Percent by volume in the vapor	1.5

19 30
Plate I. Rear View of Test Apparatus,
Part of Hoover's Mechanism



430

Boiling point at 1 atm of pressure, °F	-21.6
Maximum boiling range, °F	0.5
Maximum high boiling impurities,	
Percent by volume	0.01
Chloride content	None
Critical temperature, °F	232.2
Critical pressure, psia.	596.8
Critical volume, lb per ft ³	0.02870

Test Section and Heating Element

A 25 1/4-in. length of Type 304 stainless steel tubing formed the test section of the system. The Freon 12 was heated in the test section by passing an electric current through the tubing. Power was supplied through leads from the transformer to two rectangular steel 10 x 4 x 1/2-in. flanges welded to each end of the test section.

The test section was connected into the loop by bolting the rectangular flanges to circular Ladish Welding Neck Flanges which were welded to the loop proper. The loop proper consists of all the segments forming the oval with the exception of the test section. Figure 3 is a detail drawing of the test section showing its attachment to the loop. The free ends of the rectangular flanges were bolted to wooden panels attached to the framework. This arrangement added stability to the loop within the frame while providing electrical insulation between the test section and the frame.

The test section was electrically insulated from the loop proper by a 1/16-in. Teflon gasket placed between the flanges at both ends of the test section. The du Pont Teflon-Tetraflouroethylene Resin is

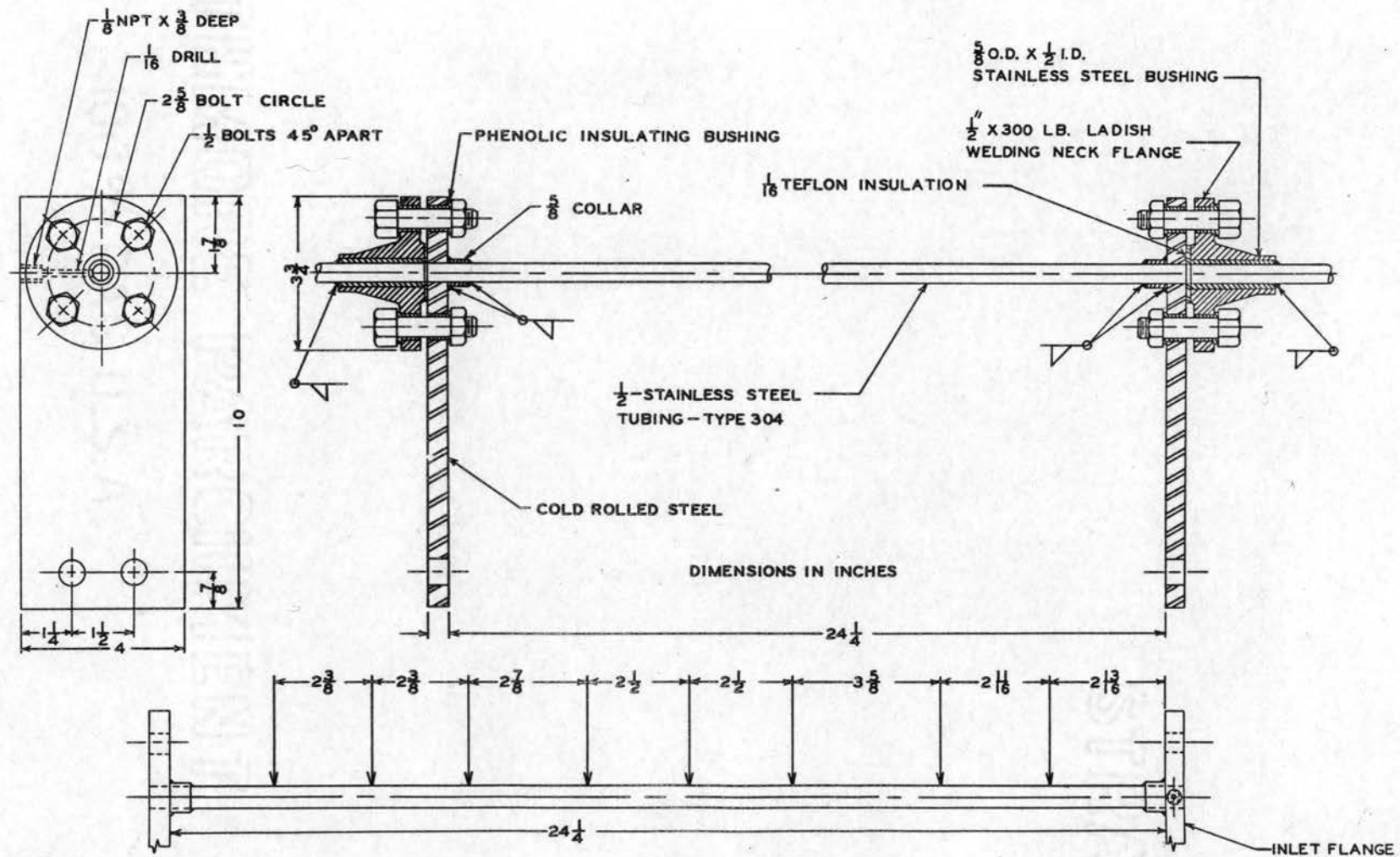


Fig. 3. Test Section Details.

completely inert to practically all known chemicals and, therefore, any danger of fluid contamination by the insulation was eliminated. Added electrical insulation was provided by placing phenolic insulating bushings in the bolt holes of the flanges.

Heat insulation was provided by wrapping the loop with a 1/8-in. layer of asbestos type followed by a 1 1/2-in. layer of fiber glass. The entire loop was then wrapped with a layer of aluminum foil to reduce radiative heat loss.

Power Supply

The electric power supply was regulated in a two-step process. Variation of the 220 volt supply voltage to values in a range of approximately 140-300 volts was accomplished by a General Electric Type MIRS-Form LK5 Induction Voltage Regulator. The primary-secondary voltage transformation occurred in a General Electric Type K Testing Transformer rated at 8 kva and having secondary voltage taps of 2, 4, and 8 volts. The secondary voltage was applied across the test section through leads connected to the rectangular flanges of the test section.

The power supply circuit was energized by a start-stop switch which was actuated by closing the master switch. A pilot light, operating on energization of the circuit provided indication of power supply to the test section. A wiring diagram of the power supply circuit appears in Fig. 4.

Heat Exchanger and Flow Control

The circulating fluid was cooled in a 1-in. nominal diameter copper

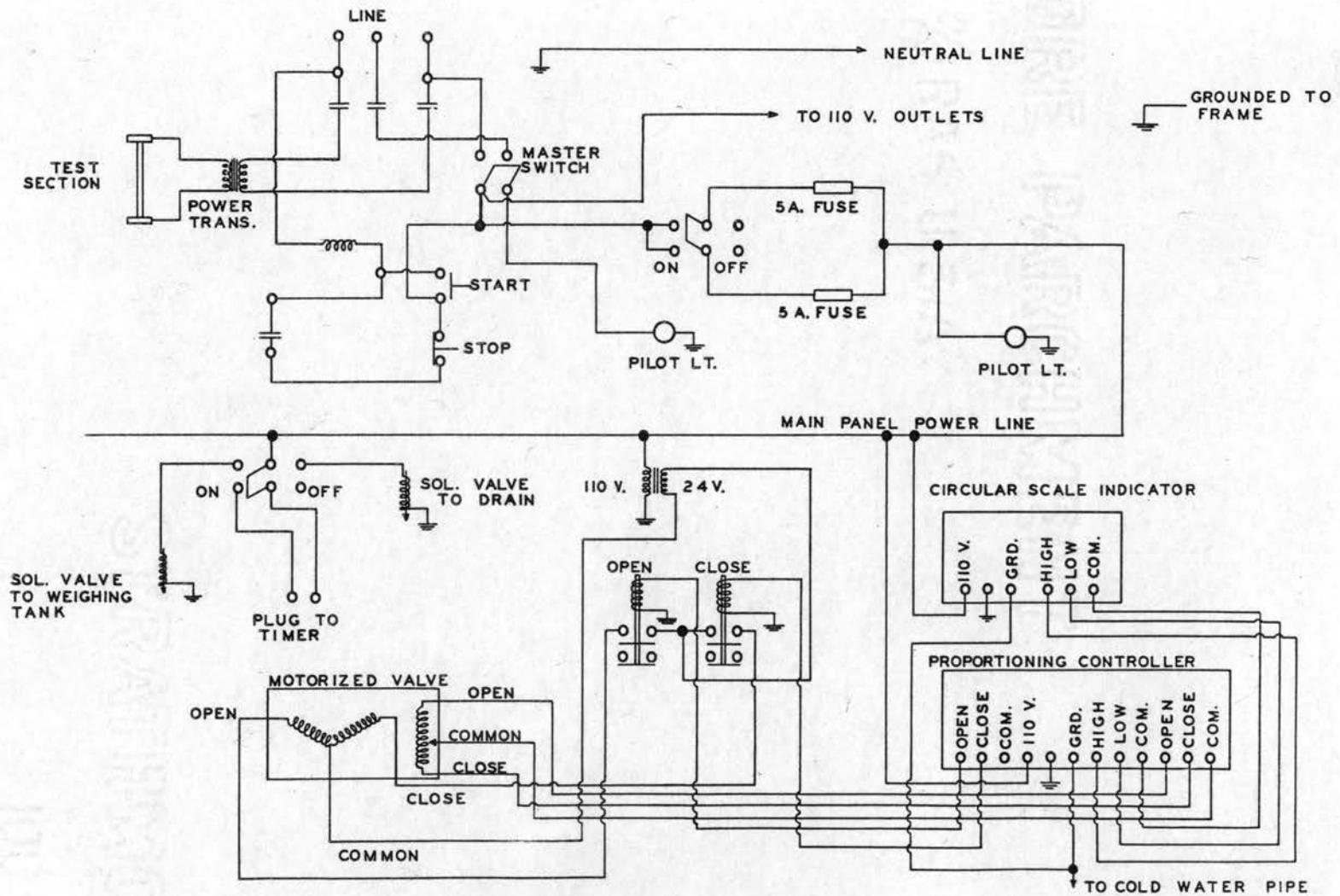


Fig. 4. Test Panel Wiring Diagram.

tubing counterflow heat exchanger 18-in. in length. The cooling fluid was tap water which entered and was removed from the heat exchanger through 1/2-in. pipe. The stainless steel tubing of the loop passed concentrically through the copper tubing, and the ends of the heat exchanger were sealed by the cap-union arrangement shown in Fig. 5.

Figure 5 shows the details of the heat exchanger.

Heat insulation was provided for the exchanger by a 2-in. thickness of "85 percent magnesia" pipe covering and a layer of aluminum foil.

The heat exchanger was divided into two equal length compartments by a 1/4-in. thick copper disk through which the stainless steel tubing passes but which prohibits passage of the cooling water. This divided arrangement allowed finer and more precise control of the fluid temperature in the loop through control of the cooling water flow. Thus, the control of the cooling water was divided into two separate and distinct circuits. A schematic drawing of the cooling water circuit is shown in Fig. 2.

In one circuit, the flow of the cooling water is regulated only by a 1/2-in. manually operated globe valve. Cooling water enters the heat exchanger at position 11, Fig. 2, and exits at position 10. The flow control of the second circuit differs from the first in that a motorized valve operating on signals from an electronic temperature controller was added. In this circuit, the flow, regulated first by a 1/2-in. manually-operated globe valve and then by the motorized valve, enters the exchanger at position 9 and exits at position 8. After leaving the heat exchanger, the two flows are recombined in the outlet piping and proceed to the drain or to a weighing tank depending on the operation of the solenoid valves.

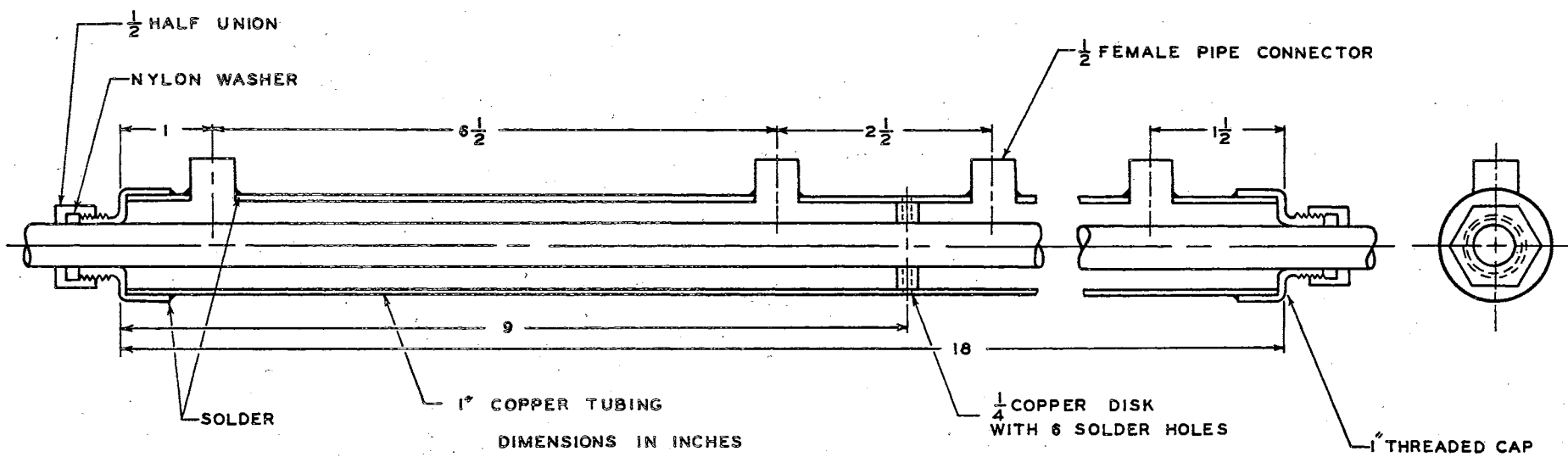


Fig. 5. Heat Exchanger Schematic.

The temperature controller was a Model 15GR16-P-13 Minneapolis-Honeywell circular scale 'Elektronik' proportional control indicating potentiometer having a 0-400°F range and a calibrated accuracy of ± 0.25 percent of the scale span. The potentiometer circuit operates on a continuous-balance principle in which a known electromotive force (emf) from a battery is varied by the movement of a contactor along a slidewire and compared with an unknown emf in a thermocouple attached to the outside of the tubing at the entrance to the test section. An electronic amplifier detects any unbalanced emf in the measuring circuit, and applies this amplified voltage to drive a balancing motor. This motor positions the slidewire contactor and rotates the circular scale so that the corresponding temperature at the test section inlet is indicated.

The tube wall temperature at the test section inlet was held constant by means of a manually adjusted set point on the electronic controller. If the temperature at the test section inlet differs from the set point temperature, there exists a voltage unbalance in the thermocouple-set point slidewire circuit. This unbalanced emf, amplified electronically, actuates the control motor which operates the valve. The motor causes the valve to open or close, thus controlling the flow of cooling water into the heat exchanger, so that the inlet temperature tends towards the set point. When the inlet temperature reaches the set point, the circuit is again in balance and the power to the motor is cut off. The valve is actuated again when the controller senses a change in the inlet temperature making it possible to hold this temperature constant.

The control motor was a Model M904E Minneapolis-Honeywell 24 volt 60 cycle Modutrol Motor. A type AT72D12CG2 Minneapolis-Honeywell

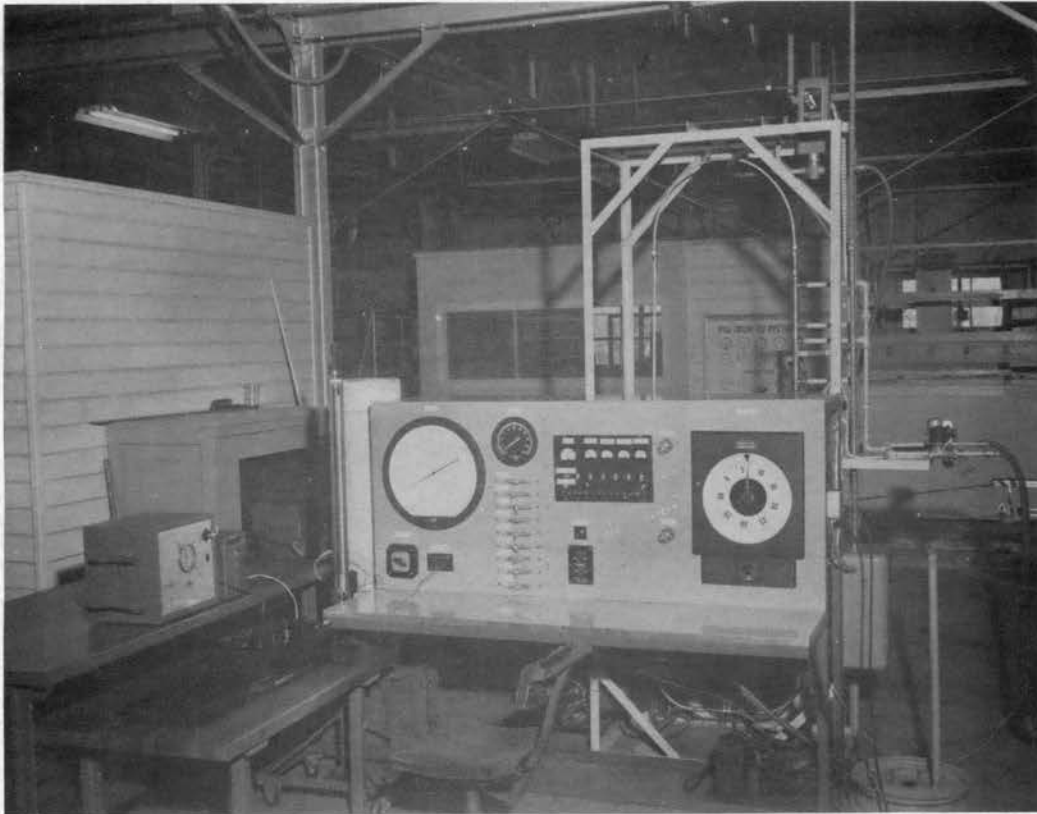
transformer with 110 volt primary was provided to supply the required operating voltage. The motor actuated the valve through a Minneapolis-Honeywell Type Q601D valve linkage. A wiring diagram of the circuits of these instruments appears in the lower portion of Fig. 4.

Instrumentation Facilities

The thermal syphon heat transfer apparatus was instrumented to make the following measurements: (A) electrical, (B) cooling water flow rate, (C) pressure, and (D) temperature. Most of the instruments necessary for these measurements were mounted on a central control panel as shown in Plate II. The various instrumentation facilities will be discussed separately according to the above listing.

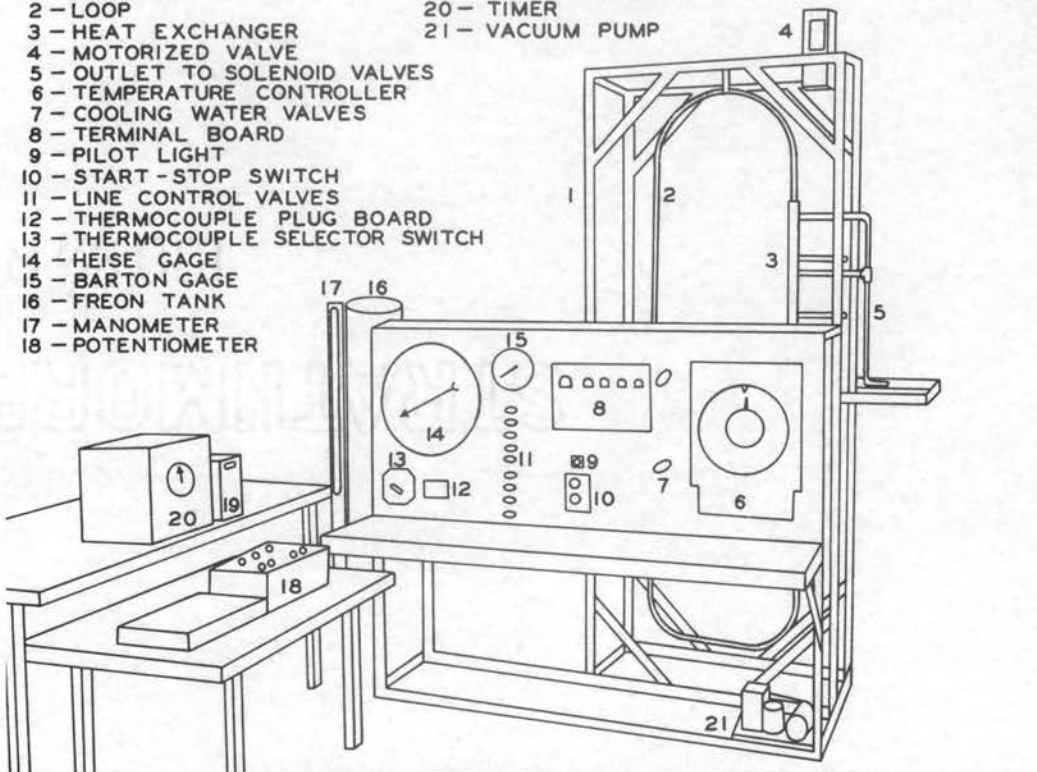
Electrical Instrumentation. The primary voltage was measured at the output of the General Electric Induction Voltage Regulator, and the secondary voltage was measured between the rectangular flanges of the test section. The indicating instruments were Triplet voltmeters. Triplet ammeters were used in conjunction with Esterline-Angus Model C 'Universal' current transformers with 160:1 ratio to indicate the current in the primary and secondary. Figure 6 is a wiring diagram of the electrical instrumentation.

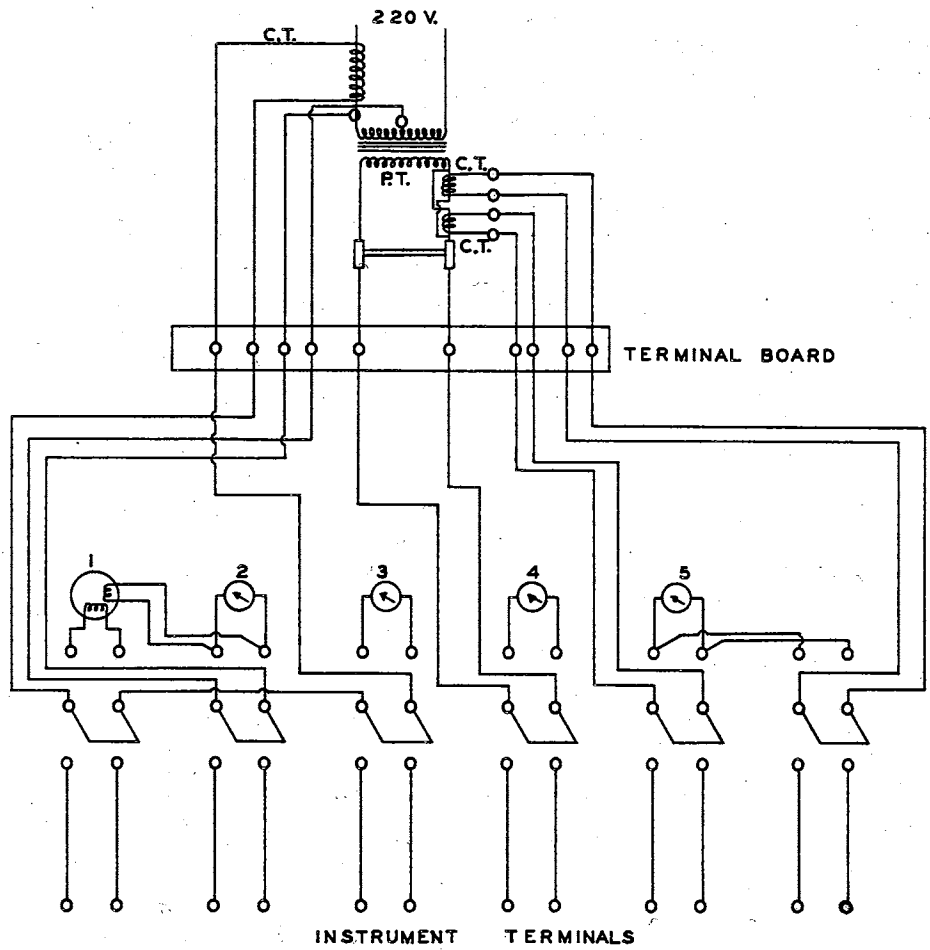
As shown in Fig. 6, the secondary current was secured using two current transformers. The circuit was so arranged such that either transformer could be switched into the measuring circuit and a separate current reading taken. The total current through the test section was obtained by addition of the reading from the two transformers using the multiplying factor of 160. This method of separate current measurements prevented overloading the indicating instruments.



LEGEND

- | | |
|-----------------------------------|-------------------|
| 1 - FRAME | 19 - GALVANOMETER |
| 2 - LOOP | 20 - TIMER |
| 3 - HEAT EXCHANGER | 21 - VACUUM PUMP |
| 4 - MOTORIZED VALVE | |
| 5 - OUTLET TO SOLENOID VALVES | |
| 6 - TEMPERATURE CONTROLLER | |
| 7 - COOLING WATER VALVES | |
| 8 - TERMINAL BOARD | |
| 9 - PILOT LIGHT | |
| 10 - START-STOP SWITCH | |
| 11 - LINE CONTROL VALVES | |
| 12 - THERMOCOUPLE PLUG BOARD | |
| 13 - THERMOCOUPLE SELECTOR SWITCH | |
| 14 - HEISE GAGE | |
| 15 - BARTON GAGE | |
| 16 - FREON TANK | |
| 17 - MANOMETER | |
| 18 - POTENTIOMETER | |





- P.T. - POWER TRANSFORMER
- C.T. - CURRENT TRANSFORMER
- 1 - WATTMETER
- 2 - 0-150 VOLTMETER - PRIMARY SIDE
- 3 - AMMETER - PRIMARY SIDE
- 4 - 0-10 VOLTMETER - SECONDARY SIDE
- 5 - AMMETER - SECONDARY SIDE

Fig. 6. Instrument Wiring Diagram.

All instruments were connected by means of double-pole double-throw switches to a terminal board mounted in back of the test panel. The use of the terminal board provided an orderly wiring arrangement and minimized the danger of short circuits. Plate III illustrates the method of panel wiring.

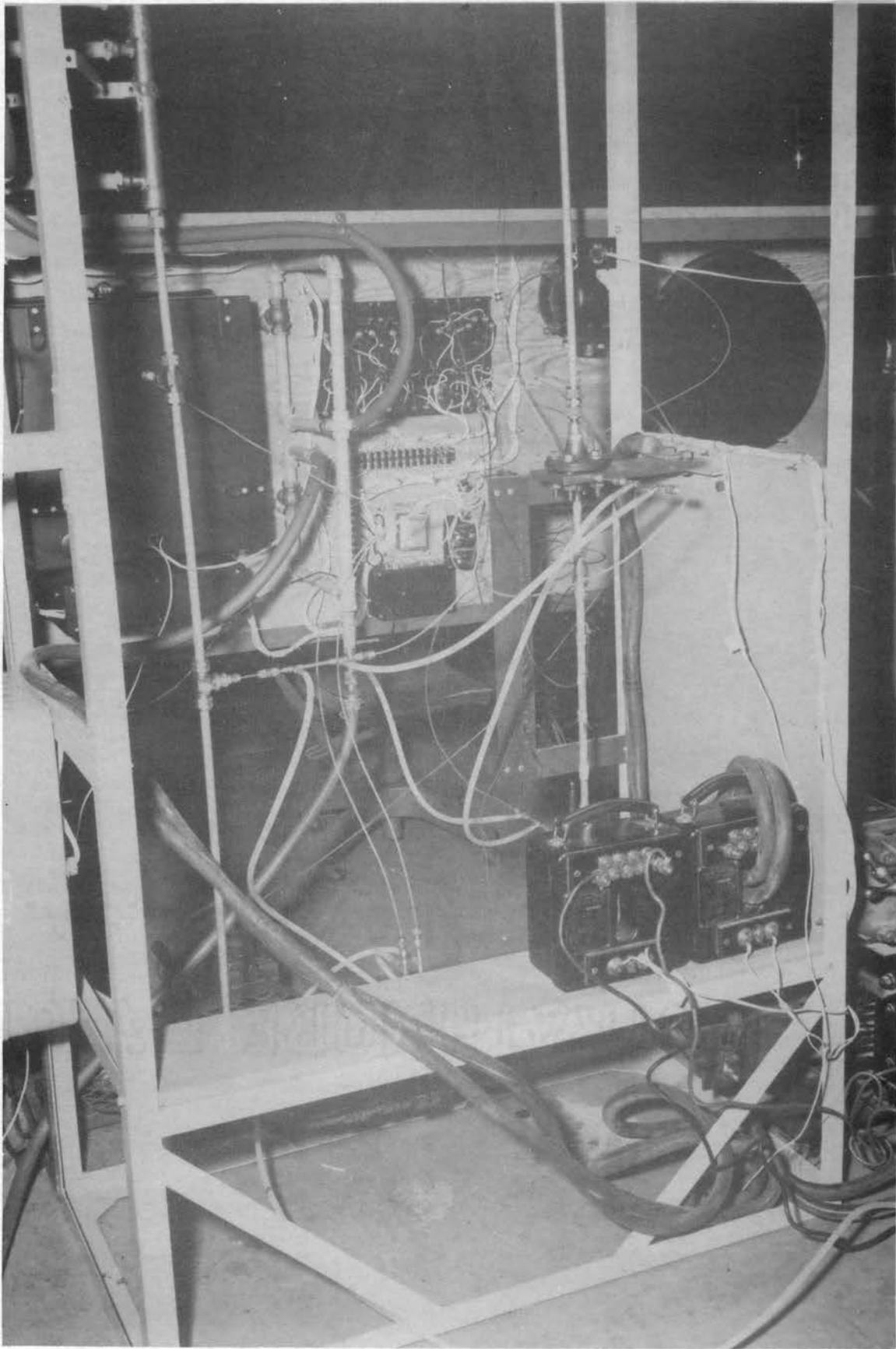
Instrument terminals for connection of precision instruments into the measuring circuit were located on a terminal board on the front of the test panel. The Triplett meters were used only for indicative or reference purposes while the precision instruments were used to make exact measurements for use in calculations. By means of the DPDT switch, either the Triplett meters or the precision instruments could be switched into the measuring circuit.

The precision instruments consisted of a General Electric AC voltmeter type P-3, 0-15 or 0-30 volt range, accuracy 0.2 percent and a General Electric AC ammeter type AP-9, 0-1 or 0-2 ampere range, accuracy 0.5 percent.

Measurement of Cooling Water Flow. The exit flow of the cooling water was controlled by two 1/2-in. type K-10-A 115 volt General Controls solenoid valves so that the flow could be diverted into either the drain or into a weighing tank.

The normally-closed valves were opened by energizing the solenoids and both valves were controlled by a single DPDT switch mounted on the test panel terminal board. The electrical circuit, shown in the left center of Fig. 4, was so arranged that one of the solenoids was energized and the other de-energized at all times when the main panel power line switch was closed. Thus, the flow could always proceed either to the weighing tank or the drain depending on the operation of the solenoids.

Plate III. Panel and Instrument Wiring.



When the solenoid valve, which allowed flow into the weighing tank, was energized, a timer was instantaneously actuated and continued to operate until the solenoid was de-energized and the valve closed. The time for any arbitrary weight of water collected in the weighing tank could then be observed and the mass rate of flow determined.

Pressure Instrumentation. The pressure instrumentation of the thermal syphon included provisions for measuring the system pressure and the differential pressure across the venturi.

The system pressure was measured at the inlet to the test section (position 3, Fig. 2) the measuring instrument being a Heise pressure gage. The pressure tap was made directly into the rectangular flange (see flange detail in Fig. 3) of the test section by a 2 1/2-in. length of 1/8-in. O.D. stainless steel tubing. The free end of the tubing was connected to a line cooler of the type shown in Fig. 7, and further connection to the Heise gage was made with 1/8-in. copper tubing. Swagelok fittings were used in assembling the pressure tap. The pressure tap was cooled by water flowing through the line cooler along the outside surface of the stainless steel tubing to insure that the instrument lines would be full of liquid. This precaution was necessary to protect the Heise gage from damage due to hot fluids.

The Heise gage was a Model H16927 Bourdon type pressure gage with a scale graduated in one-psi increments from 0-1000 psi and a calibrated accuracy of 0.1 percent of the full scale reading.

The flow rate of the test fluid was determined by measuring the pressure drop across a calibrated stainless steel venturi. Details of the venturi are shown in Fig. 8.

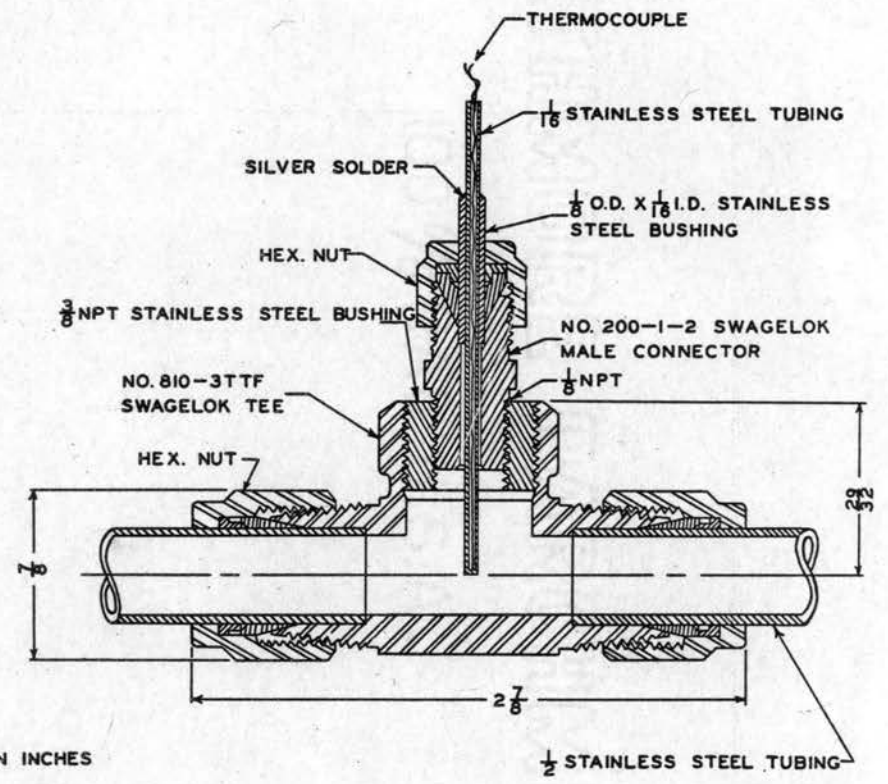
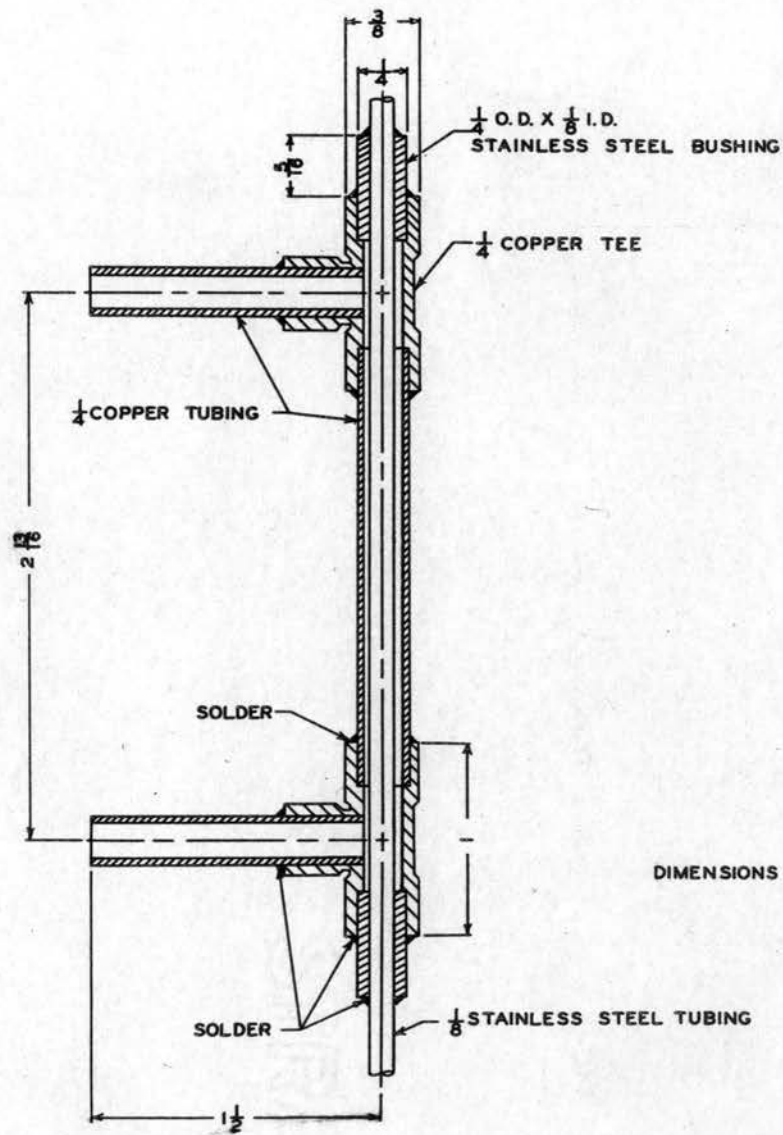


Fig. 7. Line Cooler and Thermocouple Well Details.

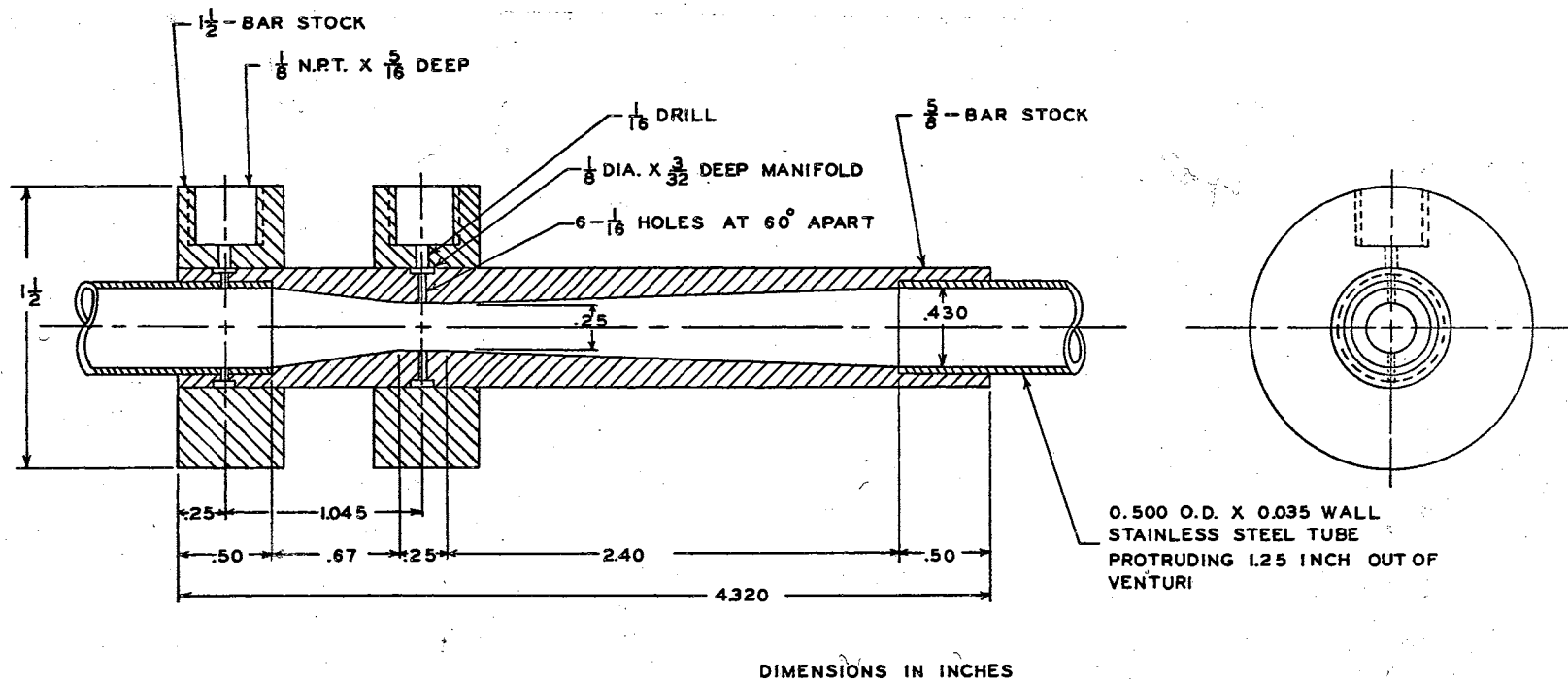


Fig. 8. Venturi Meter.

One pressure tap was located at the throat and another 1.045-in. upstream of the throat. The taps were connected to the venturi as already described and line coolers were used to cool the fluid. As shown in Fig. 8, a $1/8 \times 3/32$ -in. manifold or piezometer ring was grooved around the circumference of the venturi at each pressure tap. The manifolds collected the pressure impulses for transmission to the measuring instrument through six $1/16$ -in. diameter holes drilled 60° apart into the venturi tube wall. This arrangement allowed an average pressure measurement to be made.

The differential pressure was measured with a Model 200 Barton double bellows type differential pressure gage having a scale graduated in 0.2-in. of water from zero to twenty inches and a calibrated accuracy of 0.5 percent of the full scale reading.

The operation of the pressure gages was controlled by $1/4$ -in. Hoke needle valves with Swagelok tube ends to accommodate the $1/8$ -in. copper tube instrument leads. The pressure gages could be completely shut off from the system by closing the needle valves which were mounted to the test panel.

Temperature Instrumentation. The inlet and outlet bulk temperatures were measured at positions 1 and 5, Fig. 2, by thermocouples inserted directly into the fluid. A Minneapolis-Honeywell Megapok Type J iron-constantan thermocouple with the measuring junction sealed inside a $1/16$ -in. diameter stainless steel tube was used to measure the temperature at these points. The thermocouple was inserted into the fluid using the Swagelok tee arrangement shown in Fig. 7. The outlet bulk temperature was measured some distance above the test section in order to ensure an average temperature measurement.

The test section outside tube-wall temperatures were measured at eight different points along the tube length. The thermocouple locations are shown in Fig. 3. . Two iron-constantan thermocouples were spot welded to the tube at each location, and were wrapped one and a half times around the tube to ensure stability and to minimize the effects of conduction from the hot end of the thermocouples. A wrapping of glass tape added to the stability of each connection. The inside tube-wall temperatures were calculated by the Kreith-Summerfield equation shown in Appendix C.

Depth thermocouples were also inserted into the loop insulation at several locations to provide a check for heat loss to the atmosphere.

Two thermopiles consisting of four junctions were used to measure the cooling water temperature differential between the inlet and outlet of the heat exchanger. The thermopile was used to multiply the normal emf developed by the small cooling water difference.

The thermocouples used in the installation were 30 gage iron-constantan thermocouples. All junctions were spot welded and coated with "Glyptal" enamel to provide insulation.

The inlet and outlet bulk temperatures and the cooling water temperature differential were measured by a potentiometer-galvanometer circuit using a Rubicon Type B potentiometer in conjunction with a Leeds and Northrup Model 2430-A galvanometer.

Figure 9 is a schematic diagram of the thermocouple measuring circuit. This circuit was so arranged that a particular temperature could be measured by plugging the iron-constantan extension wire from the potentiometer into the corresponding circuit using a Minneapolis-Honeywell "Quik Konnect" plug board and jack plugs.

The insulation temperature and the test section wall temperatures (below 600°F) were measured by a Minneapolis-Honeywell Model 153X65 multi-point temperature recorder with a 0-600°F range. Tube wall temperatures above 600°F were measured with the Rubicon potentiometer using a thermocouple selector switch connected in parallel with the thermocouples and the plug board. Since two thermocouples were located at each point (shown in Fig. 3) on the test section tube wall, one was connected to the electronic recorder and the other to the potentiometer.

The cold junction was placed in an ice bath maintained in a Dewar flask. The thermocouple was inserted in a glass tube filled with acid-free diesel fuel and suspended within the flask.

CHAPTER V

OPERATING CONSIDERATIONS

A detailed description of a particular test procedure for a specific experiment will not be presented since the uses of the thermal syphon are several in number. A particular use of the heat transfer loop may require the development of new or slightly different test procedures depending on its application. Instead, the object of this chapter is to describe certain considerations taken in operating the heat transfer loop and preparing the measuring instruments. This information will be presented in the following order: testing for leakage, preventing tube overheating, varying operating conditions, preparation of the instruments, obtaining a vacuum, charging the loop, and indication of the steady state.

In testing for leakage, prior to the beginning of experimental work, the loop was filled with compressed air at a pressure of 900 psia and left in this condition for a period of three days. Observations of the Heise pressure gage, during this period, indicated that the system was pressure tight. Slight fluctuations in pressure were noticed but these were caused by changes in room temperature not by leaks in the system. It was possible, using this same procedure, to check the apparatus for leaks from time to time by evacuating the Freon and charging the loop with compressed air.

The possibility of tube overheating arose during operation of the thermal syphon. Overheating of the test section due to a low rate of heat transfer to the Freon or from other causes was detrimental because of the possibility of tube burnout or the occurrence of leaks in the heat exchanger or tube fittings.

Tube overheating would occur if the charge of Freon in the loop was insufficient to facilitate the necessary rate of heat transfer as the density of the Freon affected the dissipation of the thermal energy produced in the test section. Danger of overheating due to an insufficient volume of Freon in the loop was eliminated by charging the system at room temperature with a volume of the test fluid so that the loop was completely full of liquid Freon. It was then possible under these conditions to reduce the charge in the system to any arbitrary amount by bleeding part of the Freon back into the supply tank.

Another factor contributing to the overheating was the control of the cooling water. It was possible that an excessive rate of cooling could lower the average temperature of the system to such an extent that over-heating due to the lower flow rate of the circulating fluid would occur. This phenomenon occurred predominantly when operating near the critical point where an increase in the cooling water flow rate necessary to maintain equilibrium caused a marked increase in the test section wall temperatures. This danger was eliminated by charging to supercritical densities and bleeding off, when necessary, as described above, and by proper use of the electronic temperature controller.

Overheating due to the decrease in the rate of heat transfer also occurred when operating in the boiling region at pressures lower than the critical. This decrease in heat transfer was more predominant at

high heating rates. By allowing the pressure to increase such that the increasing wall temperature did not approach the saturation value, it was possible to reach the critical point without the occurrence of boiling.

As the test section was heated, the pressure in the system increased. The rate of pressure increase and the maximum pressure could be controlled by bleeding part of the charge back into the supply tank. At a constant charge, these variables could be controlled by varying the heat flux. Since the maximum pressure in the loop could not exceed 1000 psi, there existed an upper limit to the power input for any constant charge of Freon. This limit was in turn affected by the rate of cooling in the heat exchanger such that the charge, heating rate, and cooling rate were interdependent and one variable was increased or decreased with corresponding control of the other two. When heating the fluid in the test section, it was necessary to begin at low heat flux, increasing to higher values by control of the voltage regulator.

The reliability of experimental data depended, in part, on the accuracy of the measuring instruments. As a result, care was taken that the instruments were properly prepared for use with the thermal syphon apparatus.

In order to obtain pressure readings in units of absolute pressure, the zero reading of the Heise gage was set to read atmospheric pressure with the system open to the atmosphere. This procedure was accomplished by the use of the dial adjuster on the front of the gage.

It was necessary to verify the zero reading of the Barton differential pressure gage with absence of flow in the system. If the gage pointer did not indicate zero flow rate, the instrument was adjusted so that accurate indication of differential pressure across the venturi was ensured.

The Hoke needle valves which controlled the operation of the Barton gage were closed, leaving the gage inoperative, during charging of the system. This procedure was necessary because of the danger of the relatively high flow rates of the Freon during the charging process exceeding the limits of the gage and resulting in damage to the mechanism.

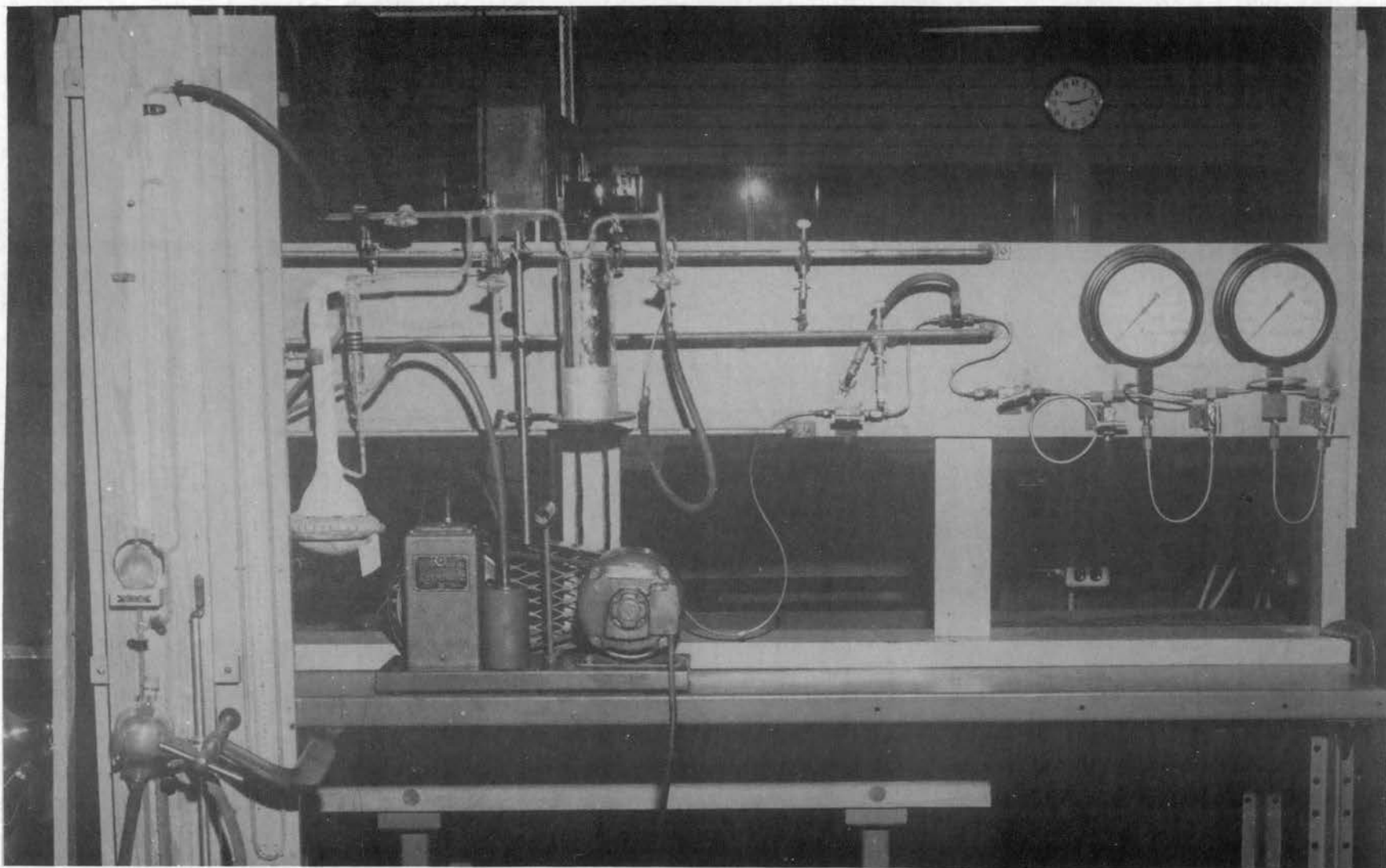
A standardization process was required in the use of the potentiometer and electronic temperature controller. The standardization of the potentiometer was quite important, especially if the charge on the battery varied, and was performed every four or five minutes when data was being recorded. The standardization of the electronic controller was not quite as critical, and was necessary only every two or three hours during continuous operation of the system.

The operation of the Modutrol control motor and valve was checked using the controls of the proportional relay to ensure their proper response to signals from the electronic controller. If the response was not satisfactory, corrections were made as indicated by the manufacturer.

Before charging the loop with Freon, it was necessary to evacuate the air and other impurities from the system. The vacuum was obtained using a Cenoco Hyvac vacuum pump operating in conjunction with a Todd mercury diffusion pump. With this arrangement, it was possible to obtain in the system an absolute pressure of sixty microns of mercury. The vacuum apparatus is illustrated in Plate IV. The McLeod gage, shown at the left in Plate IV, was used to measure the vacuum.

The Freon in the supply tank was in the wet vapor state at room temperature. To charge the loop with fluid, the supply tank was heated by two 500 watt Photospot photographic lamps so that the pressure in

Plate IV. Vacuum Apparatus.



the tank was greater than the saturation pressure corresponding to the temperature of the loop. By charging the system to a pressure of 15 to 20 psi above this original saturation pressure, the loop was completely filled with liquid. When the charging valve was opened, the initial flow of Freon into the lower pressure system was flashed into vapor, but with the addition of more Freon and the subsequent pressure increase, the vapor in the loop was compressed. This compression of the vapor was followed by condensation such that the loop was entirely filled with liquid at the completion of the charging process. With the room temperature at 70°F, the saturation pressure of Freon 12 is about 85 psia so a pressure of 100 psia in the system at this same temperature was necessary to satisfy the charging requirements. Correspondingly, at a room temperature of 80°F, the saturation pressure is 99 psia. Thus, the loop would have to be charged until a system pressure of 114 psia was reached.

Since the experimental data was recorded with the system in equilibrium, it was first necessary to establish a steady state at any particular value of set point temperature, pressure, charge, etc. The three indicators of equilibrium in the system were the electronic controller, the system pressure, and the record of the tube wall temperatures all of which remained constant when the steady state was attained. The most indicative of the three was the record of the tube wall temperatures.

CHAPTER VI

CALIBRATION OF EQUIPMENT

Most of the precision instruments used in conjunction with the heat transfer apparatus were provided with calibration curves by the manufacturer, and additional calibration was required only for the venturi, thermocouples, and the electronic temperature recorder. Each of these calibrations will be discussed separately.

Venturi Calibration

The venturi calibration consisted of determining the venturi discharge coefficient by measuring the pressure drop across the meter caused by a fluid of known flow rate. Knowing the pressure drop and flow rate, it was possible to calculate the discharge coefficient by the following equations:

$$Q = C_v A_t \sqrt{\frac{2g \Delta p}{1 - (d_t/d_i)^4}}, \quad \text{VI-1}$$

in which,

- Q = volumetric flow rate, cfs;
- C_v = coefficient of discharge;
- A_t = venturi throat area, ft²;
- d_t = venturi throat diameter, ft;
- d_i = inside pipe diameter, ft;
- Δp = pressure differential, ft of flowing fluid; and
- g = gravitational constant, ft per sec².

The calibrated venturi was then used to measure the flow rate of the circulating fluid in the loop by inserting the measured pressure differential and the predetermined value of the discharge coefficient into Eq. VI-1, and calculating the flow rate.

The venturi was calibrated using water instead of Freon for reasons of simplicity as it was not necessary to contain the fluid. The arrangement of the calibration apparatus is shown in Fig. 10.

The flow rate was controlled by the valving shown in Fig. 10. The valve upstream of the venturi remained in the open position while the flow rate was varied by the needle valve located downstream providing undisturbed flow through the venturi.

The mass flow rate was determined by the previously-described weighing tank method in which the flow was diverted from the drain into a weighing tank by the solenoid valves for a measured time interval. Knowing the mass rate of flow and the water density, it was possible to obtain the volumetric flow rate.

Water temperature was measured at the outlet of the flow line in the drain, and any temperature difference between the point of measurement and the throat was assumed negligible. The physical properties of water were evaluated at this temperature.

The differential pressure was determined by connecting the venturi pressure taps to a manometer using as the measuring liquid either water or Meriam No. 3 manometer fluid with a specific gravity of 2.95. Water was used at the lower flow rates to make possible more precise readings and was replaced by the Meriam fluid at higher flow rates. The pressure differential obtained when using the Meriam fluid was converted to ft of H₂O for insertion into Eq. VI-1.

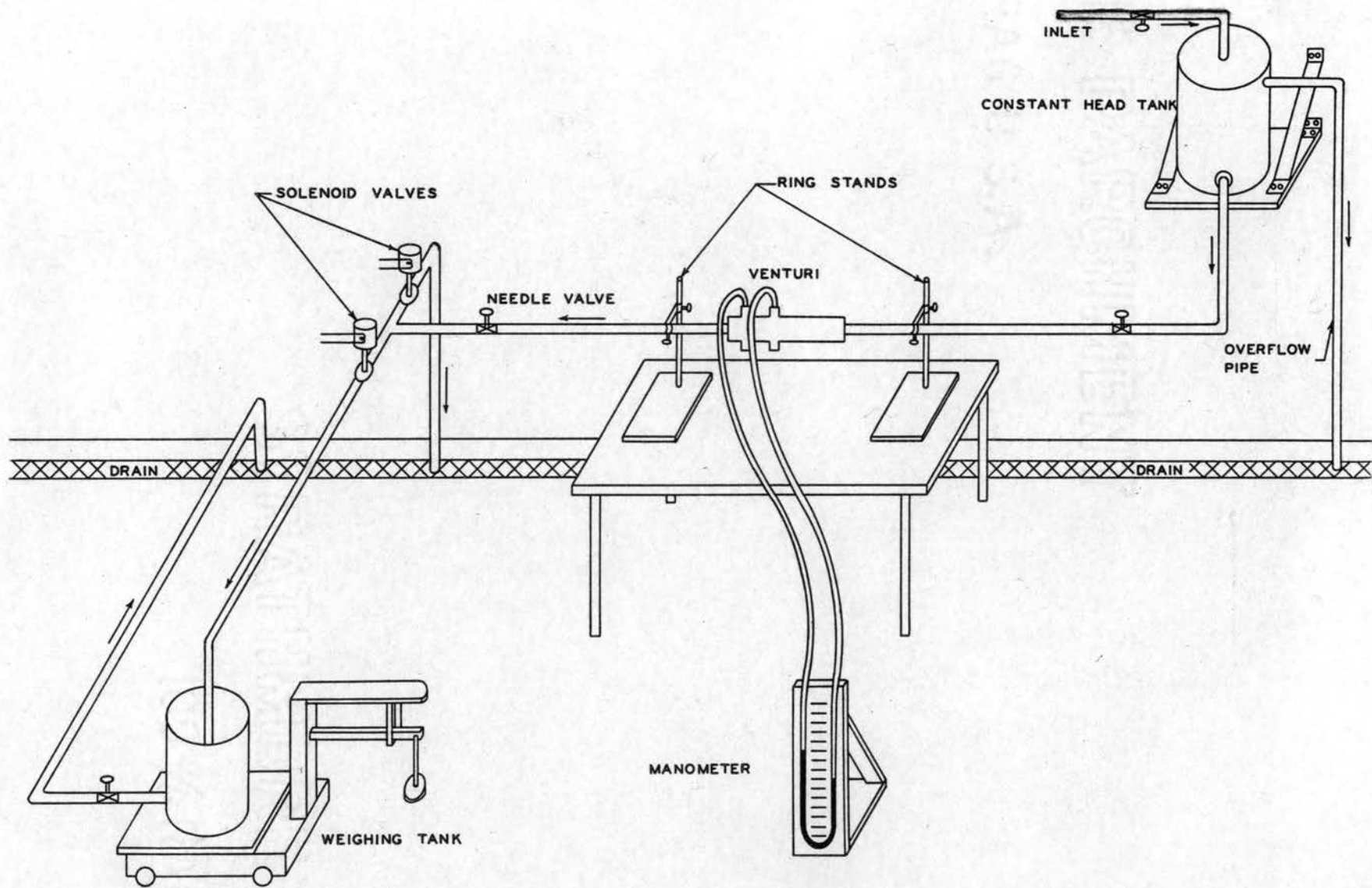


Fig. 10. Venturi Calibration Setup.

Provisions for water supply were made by connecting the venturi to a constant head tank as shown in Fig. 10 or by direct connection to the municipal water line. Using the municipal water line directly, it was possible to obtain flows with Reynolds numbers as high as 2.65×10^4 , considerably higher than the 1×10^4 maximum obtainable with the constant head tank. However, the use of the municipal water line presented an impediment to obtaining the desired calibration accuracy because of the accompanying pressure surges common to all such installations. These pressure surges were clearly evident when observing the manometer as the heights of the menisci varied as much as an inch throughout any particular run in which the flow rate was held constant. As a result, several readings were taken during each run, and the average pressure differential determined. These pressure surges were especially troublesome at low flow rates where accuracy was inobtainable, and more seriously affected the water than the greater density Meriam fluid.

By using the constant head tank as the water supply, it was possible to eliminate the pressure surges and hold the manometer level constant during a run. This was especially useful at low flow rates. However, because the height of the tank was only about 30 ft, the maximum flow rate was limited and proved to be a little less than half that obtained using the municipal water line.

A check of flow conditions during the calibration runs was made by plotting the mass flow rate (lb per sec) against pressure drop (ft of H_2O) on log-log paper. A straight-line plot was obtained from which it was possible to check the validity of the observed data. Any run for which the data were not coincident with the straight-line plot was considered inaccurate and repeated.

Since the discharge coefficient is a function of Reynolds number at low values of the dimensionless parameter, it was possible to represent the calibration data by a C_v vs Re plot as shown in Fig. 11.

As seen in Fig. 11, the scattering of data was quite pronounced in the regions of $Re > 10,000$ and $Re < 3000$. No data using the constant head tank as a source were obtained for $Re > 10,000$ and the scattering in this region was attributed to the pressure surges. The scattering of data in the region $Re < 3000$ was even more pronounced, and results obtained in this region were completely unreliable. This phenomenon was attributed to two causes. At low flow rates where the difference in the level of the two columns of manometer fluid was small, the readability of the instrument was unsatisfactory and it was difficult to obtain an accurate pressure differential. Also, the lower portion of the curve falls in the region in which the flow is undergoing the transition from laminar to turbulent flow. According to Lee and Sears (8), this region occurs at $2100 < Re < 3100$. The instability of this transition range rendered accuracy an impossibility as the venturi was unreliable in this region.

At sufficiently high Reynolds numbers, the C_v vs Re curve becomes asymptotic to the horizontal such that the discharge coefficient becomes independent of the Reynolds number and approaches a constant value of 0.97. According to Jorissen (9), this is the coefficient of calibration to be used in Eq. VI-1. The use of $C_v = 0.97$ was justifiable in determining the flow rate of the Freon in the thermal syphon loop as the Reynolds numbers were high enough that the discharge coefficient could be considered constant. An exact value of C_v for the low Reynolds number range could be calculated by a trial-and-error process using the pressure drop to obtain the proper ($C_v - Re$) relation. This process was necessary as it was impossible to measure the velocity of the fluid in the loop directly.

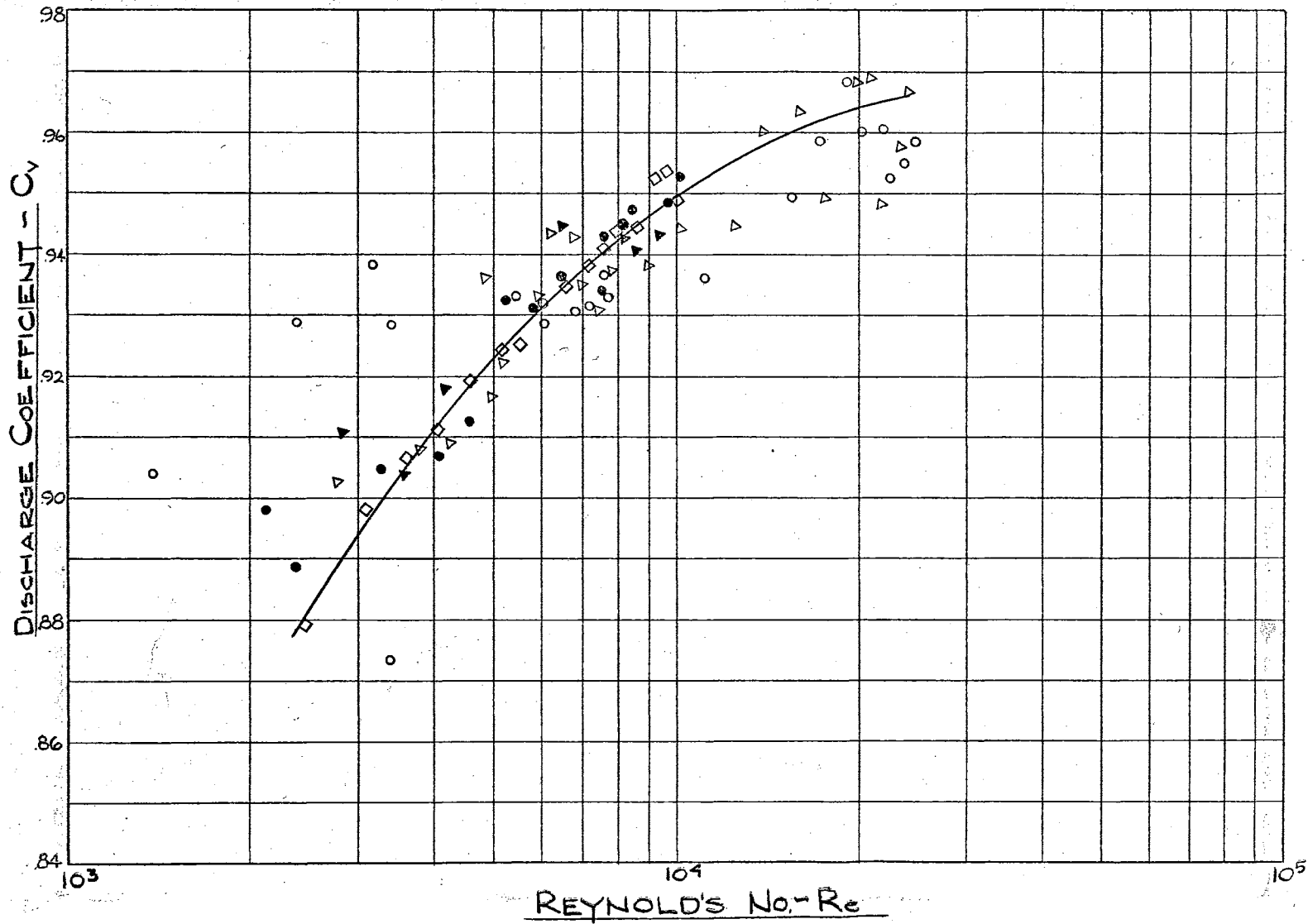


Fig. 11. Venturi Calibration Curve.

Thermocouple Calibrations

The thermocouple calibrations consisted of measuring the emf generated by the iron-constantan thermocouples using junctions at known temperatures. The measured values of emf were compared with values given in the National Bureau of Standards reference tables, for the particular temperatures, to determine a suitable correction. By measuring the emf generated at several known temperatures, it was possible to obtain a calibration curve for use in determining true temperature values from the potentiometer readings.

Calibration data were obtained at the freezing and boiling temperatures of water and the freezing temperatures of pure samples of tin, lead, and zinc. The metals and corresponding freezing temperatures were certified by the National Bureau of Standards and are listed in Table I. The freezing temperatures listed are those defined by the International Temperature Scale of 1948. (10).

TABLE I
NATIONAL BUREAU OF STANDARDS FREEZING POINT SAMPLES

Material	Sample	Freezing Temperature	
		°C	°F
Tin	42e	231.9	449.42
Lead	49d	327.4	621.32
Zinc	43f	419.5	787.10

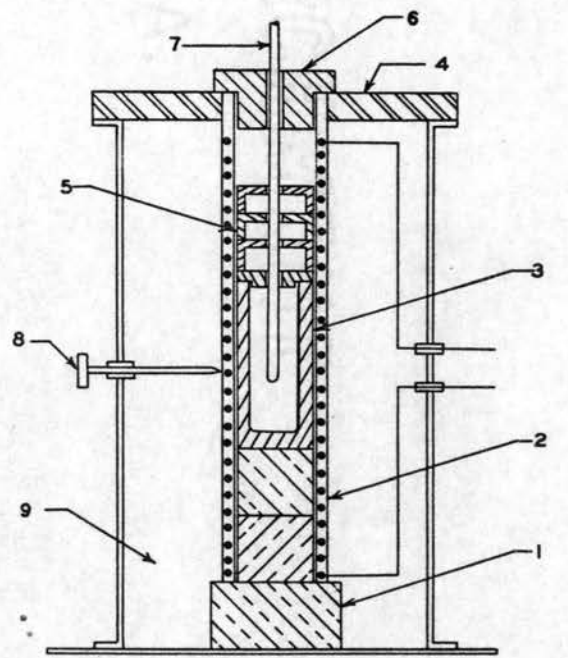
Two separate calibrations were required; one for the Magapok or bulk temperature thermocouples, and the other for the tube wall

thermocouples. Because of their respective uses, it was necessary to calibrate the Megapok thermocouple only up to the tin point while the tube wall thermocouple wire was calibrated to the zinc point since the wall temperatures were much higher than the fluid bulk temperatures.

All electrical measurements were made by the same potentiometer and galvanometer previously described such that the indicating instruments were calibrated simultaneously with the thermocouple wire.

With the reference junction at the ice-point, the emf generated at the boiling point of water was determined by placing the hot junction in a pyrex tube the closed end of which was immersed in a water filled vessel. Heating was provided by an electric heater and suitable shielding was used to eliminate erroneous radiation effects. The emf was measured at the occurrence of intense boiling. The boiling temperature at atmospheric pressure was determined from Keenan and Keyes' "Steam Tables" (11) after suitable corrections for the vapor pressure in the atmosphere had been made.

The freezing temperatures of the metal samples were attained by heating the samples in an electrical resistance crucible furnace designed and built by Clark (10) in the CSU Mechanical Engineering Laboratories. The furnace was designed so a uniform temperature could be obtained in the crucible zone while maintaining a suitable atmosphere in the heating section to prevent contamination of the sample. The furnace coil was designed on the basis of using 110 volt alternating current and the heat output of the coil was controlled by a variable transformer. A schematic diagram of the furnace and the calibration circuit is presented in Fig. 12. The same circuit was used for the boiling water except the furnace and variable transformer were replaced by the electric heater.



- 1 - ARMSTRONG A-20 BRICK
- 2 - HEATER ASSEMBLY
- 3 - GRAPHITE CRUCIBLE
- 4 - ASBESTOS BOARD
- 5 - GRAPHITE SHIELD
- 6 - A-20 LID
- 7 - THERMOCOUPLE PROTECTOR TUBE
- 8 - MONITORING THERMOCOUPLE ASSEMBLY
- 9 - SILOCEL INSULATING POWDER

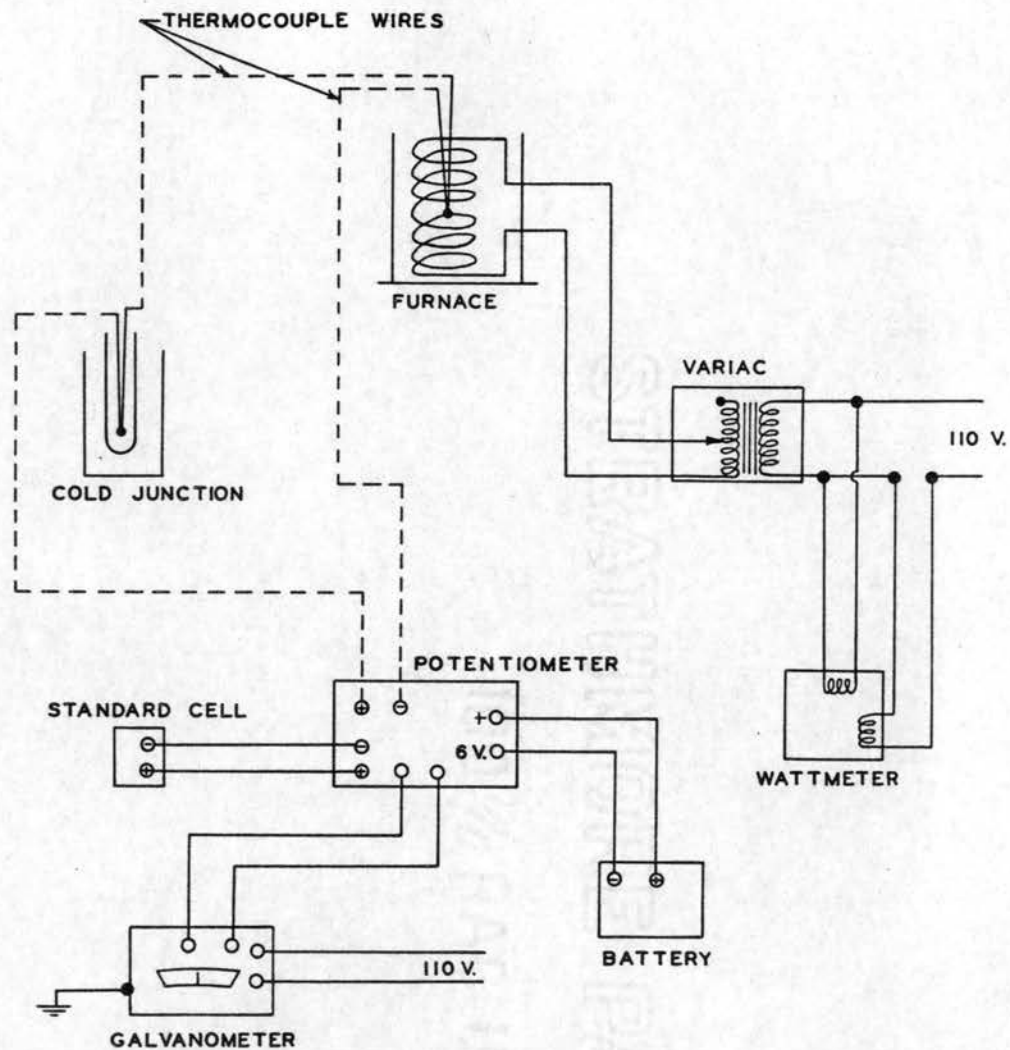


Fig. 12. Thermocouple Calibration Circuit and Furnace.

The samples were melted and allowed to freeze in the furnace according to the procedure recommended by Clark. (10). Metal samples were placed into the furnace in graphite crucibles and the hot junction, protected by a pyrex tube, was inserted into the crucible as shown in Fig. 12. As the metal melted, the tube was pushed into the center of the molten mass.

Potentiometer readings of the decreasing emf produced by the cooling samples were taken at intervals of one or two minutes until a constant reading over a prolonged time interval was observed. This constant reading indicated the freezing point of the metal. It was not necessary to plot the time vs emf cooling curves as described in reference (10); however, the data were recorded. The freezing points were clearly defined by the constant potentiometer readings which were maintained for a period of 15 to 20 minutes.

By comparing the measured values of emf with the values given in the National Bureau of Standards (NBS) Table, it was possible to obtain a correction factor by use of the following equation:

$$\text{Correction (mv)} = E_s - E_p, \quad \text{VI-2}$$

in which, E_s = emf from NBS tables, millivolts; and

E_p = measured emf at same temperature, millivolts.

The correction curves, Figs. 13 and 14, were then obtained by plotting the correction factor vs potentiometer reading. These correction factors were applied by algebraic addition to the potentiometer readings. A straight line plot was used instead of a continuous curve to facilitate linear interpolation. According to Sweeney (12), it is common practice to plot a calibration curve of this type as a broken line instead of a smooth curve especially if the deviations are reproducible. Subsequent

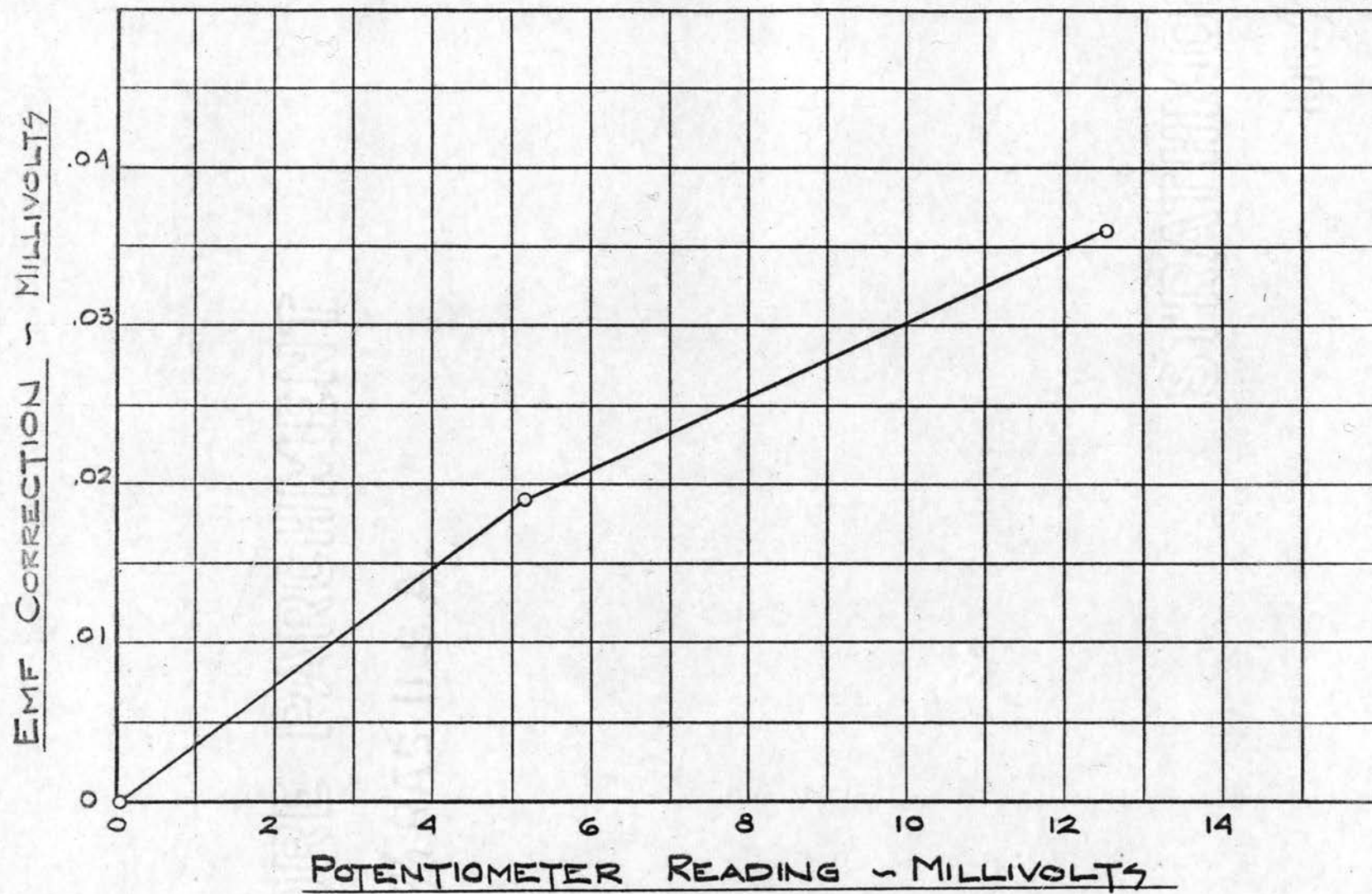


Fig. 13. Bulk Thermocouple Calibration Curve.

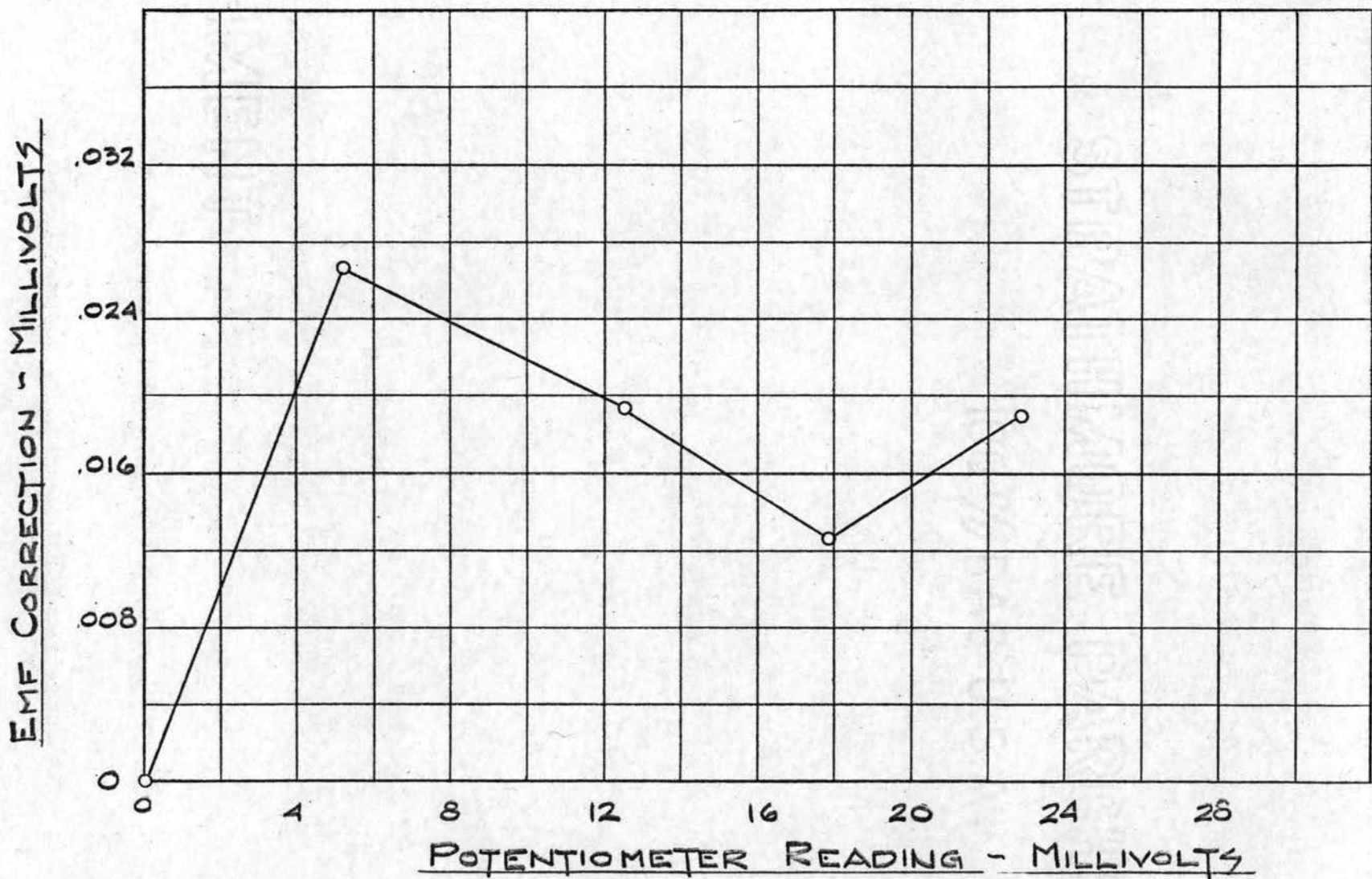


Fig. 14. Wall Thermocouple Calibration Curve.

tests of the same metals verified the reproducibility of the deviations. Since a temperature difference of 1°F is represented by an emf of approximately 0.03 mv using iron-constantan thermocouples (from NBS Tables), the error in using a broken line instead of a smooth curve was negligible. This statement may be verified by a study of the exaggerated scale of the calibration curves.

To facilitate direct calculation of temperatures from potentiometer readings, the following relationship may be used:

$$T = a + bE + cE^2, \quad \text{VI-3}$$

in which, T = temperature, °F;
 E = electromotive force, millivolts; and
 a , b , and c are constants to be determined.

The second order term proved to be negligible in the range of desired accuracy and Eq. VI-3 was reduced to the linear relationship:

$$T = n + mE, \quad \text{VI-4}$$

in which n and m are constants.

A separate and distinct linear relationship using Eq. VI-4, was calculated for each temperature region investigated to promote greater accuracy. The constants were evaluated for each region and the results are presented in Table II.

Calibration of Temperature Recorder

Since two identical thermocouples were spot welded to the test section tube wall at each location shown in Fig. 3, it was possible to connect one to the electronic temperature recorder and the other to the

TABLE II
THERMOCOUPLE CALIBRATION EQUATIONS

Temperature Range	Equation
Megapok Thermocouples	
32°F to H ₂ O boiling temp	$T = 34.30E + 32$
H ₂ O boiling temp to tin freezing temp	$T = 32.69E + 40.31$
Tube Wall Thermocouples	
32°F to H ₂ O boiling temp	$T = 34.34E + 32$
H ₂ O boiling temp to tin freezing temp	$T = 32.58E + 41.14$
Tin freezing temp to lead freezing temp	$T = 32.47E + 42.43$
Lead freezing temp to zinc freezing temp	$T = 32.65E + 39.21$

potentiometer. The calibration of the recorder consisted essentially of comparing the temperature indicated by the recorder with the temperature measured by the calibrated potentiometer to obtain a suitable correction factor.

The test section was used as the heating element and simultaneous readings of the potentiometer and recorder were made at 50° intervals with both increasing and decreasing temperature from 100 to 550°F.

Since the reference junction of the thermocouple was at room temperature instead of the ice point, it was necessary to correct the potentiometer reading by addition of the emf corresponding to ambient temperature. This corrected emf was converted to temperature and its difference from the indicated recorder temperature obtained. The average temperature difference at a particular temperature level was then corrected for thermocouple errors using the thermocouple calibration curve, Fig. 14, and converting the thermocouple correction to temperature. This conversion

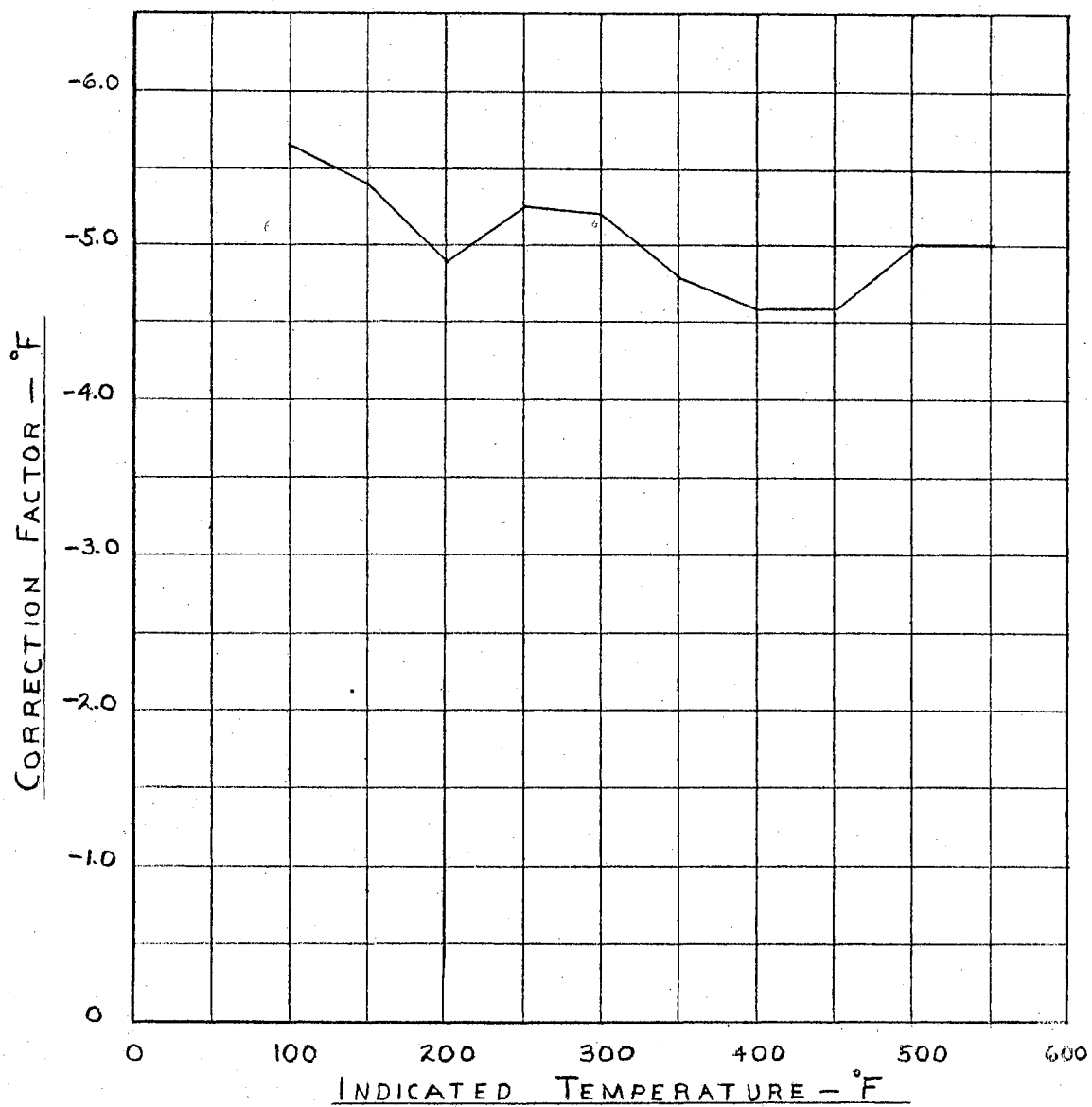


Fig. 15. Temperature Recorder Calibration Curve.

was facilitated by the fact that a thermocouple correction of 0.03 mv is equal to 1°F. This corrected temperature difference was used as the correction factor and a calibration curve was plotted (Fig.15). As seen in Fig. 15, the mean correction is approximately -5°F. This mean value was used as a constant correction factor throughout the temperature range of the recorder with sufficient accuracy. The correction factor was applied by algebraic addition to the temperature indicated by the recorder.

CHAPTER VII

SUMMARY AND CONCLUSIONS

The design presented herein has resulted in the construction of an experimental loop which has proven effective in making preliminary investigations of heat transfer phenomena in a thermal syphon type apparatus. Although the operating range of this particular loop is limited as regards maximum allowable pressure, temperature and heat flux, the satisfactory operation of the system and auxiliary equipment emphasizes the feasibility of continuation of this particular phase of heat transfer research. An advantage of the thermal syphon lies in the elimination of circulating pumps from the system and the possibility of sealing the fluid in the loop.

The possibility of using the thermal syphon apparatus as an effective heat exchange mechanism suggests continued research with different type fluids, particularly water, in order to determine optimum heat transfer characteristics and design factors. Naturally, the design of such a system will have to be modified as the operating pressures and temperatures increase.

Although the system under consideration was designed primarily for investigations in the critical regions of fluids having low critical constants, it seems feasible to investigate heat transfer characteristics in both the boiling and liquid regions for a variety of fluids.

The following observations and suggestions are presented which may be of value in future modifications and/or operation of the thermal syphon.

1. The use of the venturi as a flow measuring device proved quite satisfactory. The relatively small head loss due to its installation into the loop emphasizes the advantage of the venturi over other flow measuring devices such as the rotameter. However, it should be pointed out that operation of the system in regions of low Reynolds numbers will accentuate the unreliability of experimental results. Accurate determinations of the venturi discharge coefficient for $Re < 10^4$ are difficult, and in the transition region such determinations are impossible.

Even smooth laminar flow should be avoided, if optimum heat transfer is desired, as the rate of transfer to streamline flow is much smaller than to turbulent flow. In industrial practice, it is almost always desirable to avoid conditions such as low liquid velocity which promote streamline flow. Hence, it is desirable to operate in regions where the discharge coefficient is independent of the Reynolds number.

2. Pressure fluctuations in a flowing fluid are detrimental to the calibration of a flow meter such as a venturi. A surge tank or other type of damping device should be used to eliminate any pressure fluctuations that might exist. The use of a constant head or overflow tank will eliminate pressure surges but the flow rate may be limited due to the height of the tank.

3. A suggestion for modification of the test section instrumentation is the location of voltage taps at regular intervals along the heater tube. This arrangement would make possible determination of the uniformity of heat flux and the degree of linearity of fluid bulk temperature variation along the test section tube.

4. During operation of the system, it was observed that control of the test section inlet temperature using the set point on the temperature

controller was quite difficult at low temperatures when the heat flux was low. At these low temperatures and low cooling rates, it was difficult to control the motorized valve. Much better control of the inlet temperature was possible at temperatures above 150°F, especially, if the power input was increased.

5. If it is desirable to obtain a more accurate determination of the heat loss to the atmosphere it is advisable to increase the number of thermocouples placed in the insulation around the loop. These thermocouples should be inserted to varying depths in the insulation and also placed on the outside surface of the insulation.

SELECTED BIBLIOGRAPHY

1. Wissler, E. H., H. S. Isbin, and N. R. Amundson, "Oscillatory Behavior of a Two-phase Natural-Circulation Loop," A.I.Ch.E. Journal, Vol. 2, (June 1956), pp. 157-62.
2. Dickerson, N. L., and C. P. Welch, "Heat Transfer to Supercritical Water," Trans. Amer. Soc. Mech. Engrs., Vol. 80, 1958, pp. 746-52.
3. Kaufman, S. J., and R. W. Henderson, "Forced-Convection Heat Transfer to Water at High Pressures and Temperatures in the Nonboiling Region," NACA Research Memorandum, RM E5 1118, November 29, 1951.
4. Kaufman, S. J., and F. D. Isely, "Preliminary Investigation of Heat Transfer to Water Flowing in an Electrically Heated Inconel Tube," NACA Research Memorandum, RM E50G 31, September 27, 1950.
5. Doughty, D. L., and R. M. Drake, "Free Convection Heat Transfer From A Horizontal Right Circular Cylinder to Freon 12 Near the Critical State," Trans. Amer. Soc. Mech. Engrs., Vol. 78, 1956, pp. 1843-50
6. Schmidt, F., F. Eckert, and V. Grigull, "Heat Transfer by Liquids Near the Critical State," AAF Translation, No. 527, Air Material Command, Wright Field, Dayton, Ohio.
7. Holman, J. P. "Heat Transfer to Freon 12 Near the Critical State in a Thermal Syphon Type Apparatus," Unpublished Ph. D. Dissertation, Oklahoma State University, 1958.
8. Lee, J. F., and F. W. Sears, Thermodynamics, Addison-Wesley, Cambridge, Mass., 1955, p. 238.
9. Jorissen, A. L. "Discharge Coefficients of Herschel-Type Venturi Tubes," Trans. Amer. Soc. Mech. Engrs., Vol. 74, (August 1952), p. 905.
10. Clark, H. T. "Design and Suitability Tests of an Electric Resistance Crucible Furnace for Thermocouple Calibration," Unpublished M. S. Thesis, Oklahoma State University, 1958.
11. Keenan, J. H., and F. G. Keyes, Thermodynamic Properties of Steam, Wiley and Sons, New York, N. Y., 1956.
12. Sweeney, R. J. Measurement Techniques in Mechanical Engineering, Wiley and Sons, New York, N. Y., 1953, p. 12.

13. Alloy Tube Division, Carpenter Steel Company, Union, N. J.,
Carpenter Stainless Tubing, 1947.
14. American Society for Metals, Metals Handbook, 1948, p. 314.
15. Kreith, F., and M. Summerfield, "Heat Transfer to Water at High
Flux Densities With and Without Surface Boiling," Trans.
Amer. Soc. Mech. Engrs., Vol. 71, 1949, pp. 805-15.

APPENDIXES

APPENDIX A

DESIGN CALCULATIONS

TABLE III

PHYSICAL DIMENSIONS OF THE LOOP

Total length of loop measured along pipe axis, in.	218.6
Test section length, in.	25.25
Distance from midpoint of test section to Midpoint of heat exchanger, in.	37.0
Outside diameter of tubing, in.	0.500
Inside diameter of tubing, in.	0.430
Wall thickness of tubing, in.	0.035
Inside surface area of test section, ft ² .	0.237
Outside surface area of test section, ft ² .	0.275
Cubic capacity of test section, in ³ .	3.67
Cubic capacity of loop, in ³ .	31.74

The following calculations refer to maximum operating conditions of the thermal syphon.

Electric current required to produce maximum heat flux of 42,000 Btu per hr ft² at an average wall temperature of 600°F

$$\text{Heat Input} = q = 42000 \times A = 42000 \times 0.237 = 9952.6 \text{ Btu per hr}$$

$$\text{Electric Power} = P = (9952.6/3412) \times 1000 = 2920 \text{ watts}$$

At an average wall temperature of 600°F, the electrical resistivity of stainless steel = $\rho = 37$ micro-ohm in. (From Fig. 17)

$$\text{Resistance} = R = \rho \left(\frac{l_t}{A} \right) = \frac{37 \times 10^{-6} \times 25.25}{\pi/4 (0.5^2 - 0.43^2)} = 0.0183 \text{ ohm}$$

$$\text{Current} = I = \sqrt{\frac{P}{R}} = \sqrt{\frac{2920}{0.0183}} = 400 \text{ amps}$$

Test section voltage drop at a heat flux of 42,000 Btu per hr ft² and average tube wall temperature of 600°F

$$P = E \times I = 2920 \text{ watts}$$

E = voltage drop, volts

$$I = 400 \text{ amps}$$

$$E = \frac{2920}{400} = 7.30 \text{ volts}$$

Cooling water flow requirements at heat flux of 42,000 Btu per hr ft² and 20°F cooling water temperature difference

$$q = \omega c_p \Delta t = 9952.6 \text{ Btu per hr}$$

$$\omega = \frac{9952.6}{1 \times 20} = 498 \text{ lb per hr}$$

$$\omega = \gamma_m A_e u \quad \text{where } A_e = \text{annular flow area of heat exchanger}$$

$$u = \frac{\omega}{\gamma_m A_e} = \frac{498}{62.2 \times \pi/4 \times 1/144 (1^2 - 0.5^2)} = 1960 \text{ ft per hr}$$

or 0.542 ft per sec

Approximation of heat loss to the atmosphere at an average tube wall temperature of 600°F and an average insulation surface temperature of 150°F

thermal conductivity of asbestos = $k_{ab} = 0.125$ Btu per hr ft °F

(approximately)

thermal conductivity of fiber glass = $k_{fg} = 0.04$ Btu per hr ft °F

(approximately)

$$q' = \frac{2\pi \Delta t}{\frac{\ln r_{ab}/r_o}{k_{ab}} + \frac{\ln r_{fg}/r_{ab}}{k_{fg}}} = \frac{2\pi (600 - 150)}{\frac{\ln 0.375/0.250}{0.125} + \frac{\ln 1.875/0.375}{0.04}}$$

$$q' = 65 \text{ Btu per hr ft}$$

At a maximum power of 3 kw, the heat loss is:

$$\frac{65 \times 25.25/12}{3 \times 3412} \times 100 = 1.34 \text{ percent of the heat input}$$

Approximation of axial heat flow

At an average wall temperature of 600°F, the thermal conductivity of stainless steel is 11.0 Btu per hr ft °F. (From Fig. 16)

The axial heat flow between two points located 3-in. apart along the tube surface can be approximated, per 100°F temperature rise, as

$$q_{\text{axial}} = k A \frac{\Delta t}{\Delta x}$$

$$= \frac{11 \times \pi (0.5^2 - 0.43^2) \times 100}{4 \times 144 \times 0.25} = 1.56 \text{ Btu per hr}$$

When compared with the heat input, the axial heat flow is negligible.

APPENDIX B

PROPERTIES OF AISI TYPE 304 STAINLESS STEEL

The following properties of Type 304 Stainless Steel were taken from reference (13) and the values plotted in Figs. 16 and 17 were taken from reference (14).

TABLE IV

PHYSICAL PROPERTIES OF TYPE 304 STAINLESS STEEL TUBING

Ultimate strength, psi	85,000
Elastic limit, psi	35,000
Elongation, percent in 2-in.	50
Rockwell hardness	B-80
Specific gravity	7.93
Coefficient of Expansion per °F	
At 60° to 212°F	0.00000953
Specific electric resistance,	
Ohms per cir mil ft at 20°C	417
Structure	Austenitic Non-Magnetic
Safe scaling temp for continuous	
Service, °F	1600
Thermal Conductivity, Btu per ft ² hr °F in.	
At 500°F	130

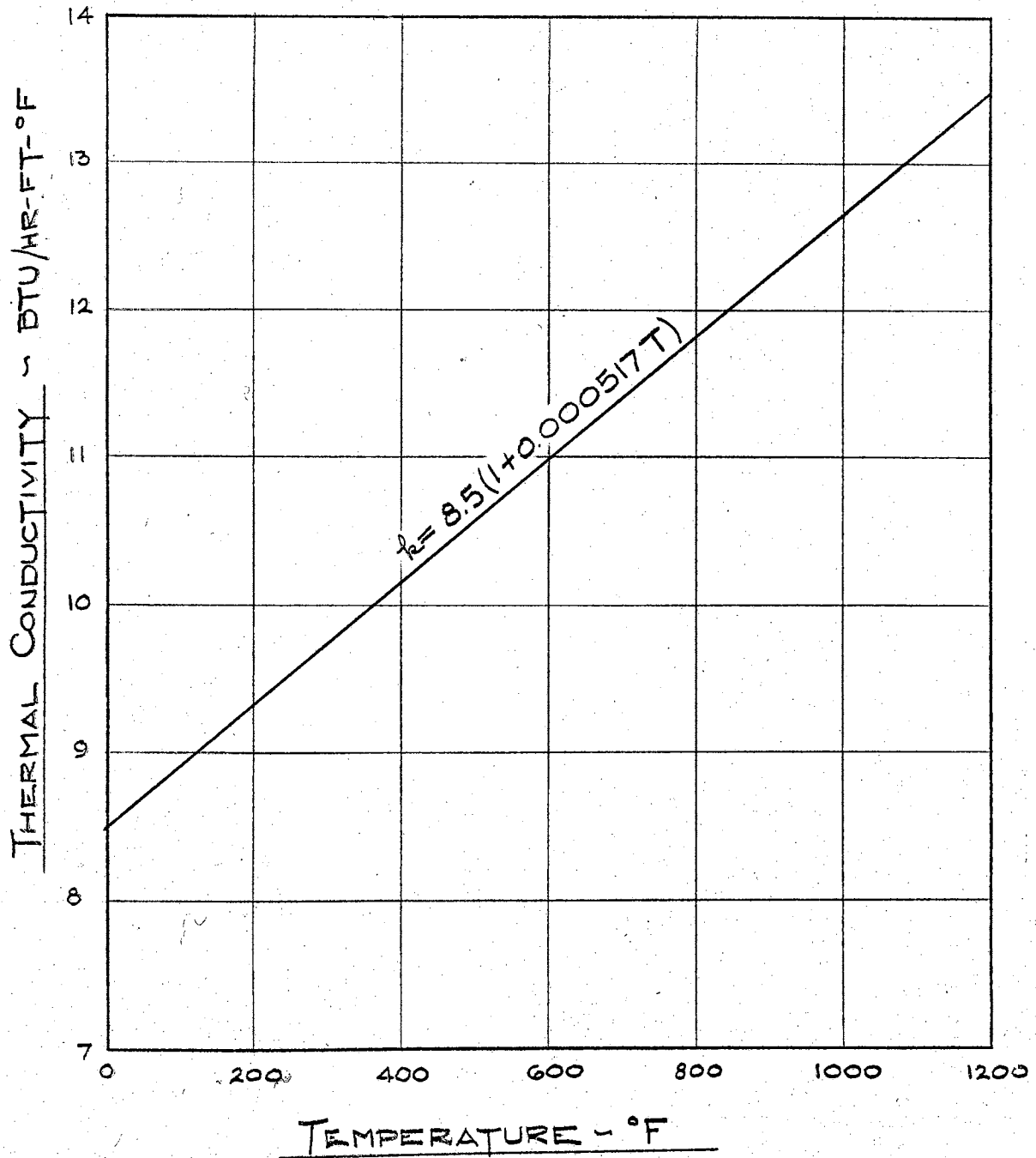


Fig. 16. Thermal Conductivity of AISI Type 304 Stainless Steel.

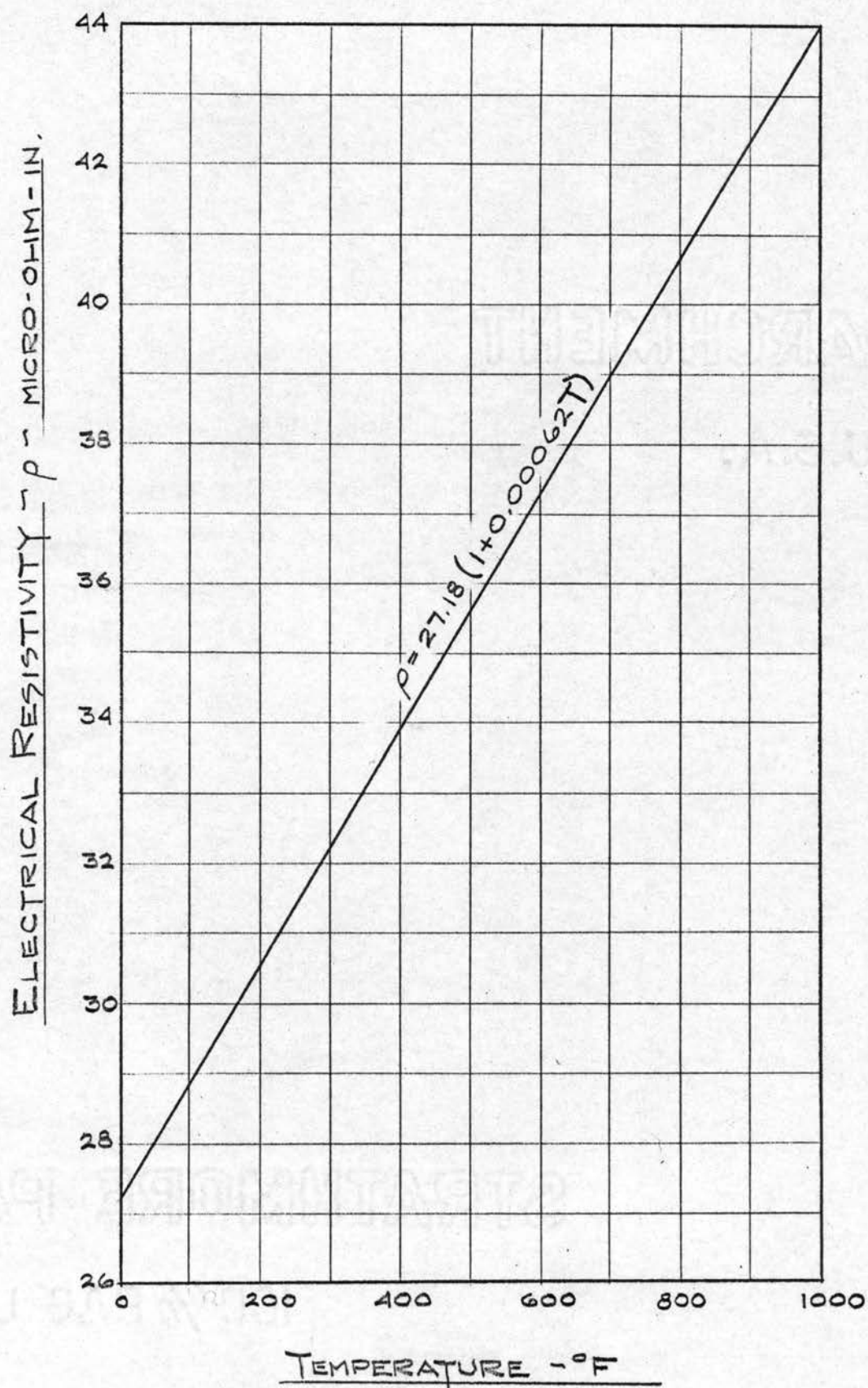


Fig. 17. Electrical Resistivity of AISI Type 304 Stainless Steel.

APPENDIX C

SOLUTIONS TO KREITH-SUMMERFIELD EQUATION

Once the outside tube wall temperatures were measured it was possible to calculate the inside surface temperatures by use of the Kreith-Summerfield equation. (15). The use of the equation provided suitable accuracy especially since the temperatures were measured to the nearest degree. The maximum error was approximately $\pm 3^{\circ}\text{F}$.

The use of the equation involved the following three assumptions.

(a) The resistivity and thermal conductivity of the tube material varied linearly with temperature.

(b) An adiabatic outer tube surface existed, i.e., heat loss through the insulation was negligible.

(c) Axial heat flow along the tube was negligible.

Assumption (a) can be verified by a study of Appendix B while assumption (b) and (c) are verified in Appendix A.

The equation derived by Kreith and Summerfield is

$$\Delta t = t_o - t_i = \frac{m}{k_o \rho_o} \left[(\Delta x)^2 + \frac{1}{3r_o} (\Delta x)^3 + (\Delta x)^4 \left(\frac{m(3\alpha + 4\alpha\beta t_o + \beta)}{6(1 + \beta t_o)(1 + \alpha t_o)} + \frac{1}{4r_o^2} \right) \right] \quad (1)$$

where,

$$m = \frac{3.413 \rho_m^2 I^2}{2\pi^2 (r_o^2 - r_i^2)^2} \quad (2)$$

ρ = electrical resistivity, ohm-ft;

- ρ_0 = electrical resistivity at 0°F , ohm-ft;
- k_0 = thermal conductivity at 0°F , Btu per hr ft $^\circ\text{F}$;
- t_0 = outside wall temperature, $^\circ\text{F}$;
- t_i = inside wall temperature, $^\circ\text{F}$;
- Δx = wall thickness, ft;
- α = temperature coefficient of electrical resistivity, $^\circ\text{F}^{-1}$;
- β = temperature coefficient of thermal conductivity, $^\circ\text{F}^{-1}$;
- I = electric current, amperes.

$$\rho_m = \rho_0(1 + \alpha t_m) = \rho_0 \left[1 + \frac{\alpha}{r_0 - r_i} \int_{r_i}^{r_0} t_r dr \right], \quad (3)$$

where, t_m = mean radial temperature, $^\circ\text{F}$; and
 t_r = temperature as a function of radius, $^\circ\text{F}$.

Insertion of the numerical constants reduces Equation (1) to

$$\Delta t = 0.4628m + 6.2647 \times 10^{-7} m^2 \left[\frac{0.002377 + 0.01282t_0}{(1 + 5.17 \times 10^{-4}t_0)(1 + 6.2 \times 10^{-4}t_0)} \right], \quad (4)$$

where, $m = 1.353 \times 10^7 \rho_m^2 I^2$, and (5)

$$\rho_m = 2.265 \times 10^{-6} (1 + 0.00062t_m). \quad (6)$$

The temperature drop across the tube wall was computed for different values of outside wall temperature and current by means of an IBM 650 computer according to the method outlined in reference (7) and the cross plot, shown in Fig. 18, was obtained.

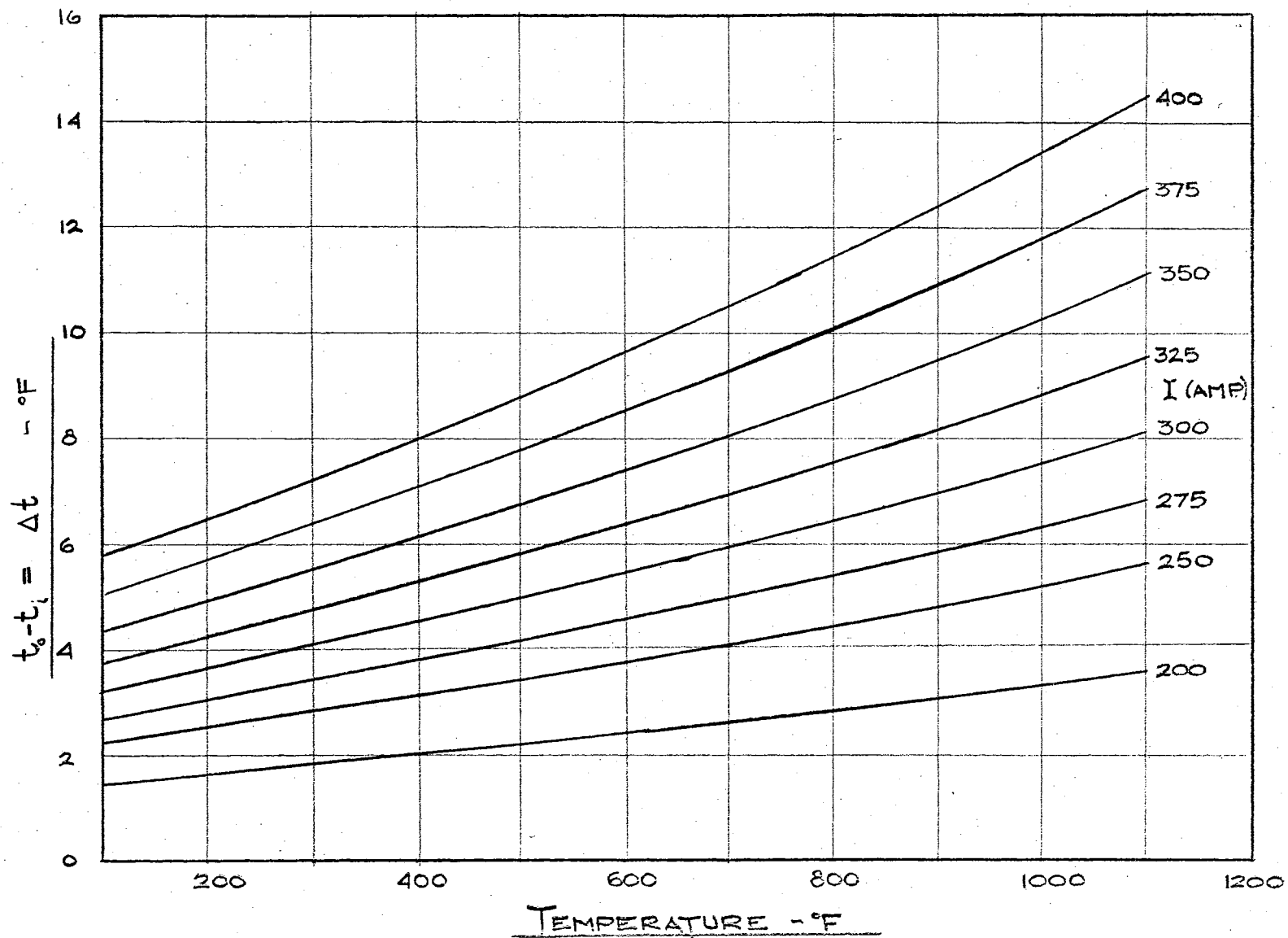


Fig. 18. Solutions of Kreith-Summerfield Equation.

APPENDIX D

SYMBOLS

A	Area, ft ²
A _d	Surface area of heat transfer element, ft ²
A _i	Inside cross sectional area of tube, ft ²
A _t	Area of venturi throat, ft ²
c _p	Specific heat capacity at constant pressure, Btu per lb °F
C _v	Venturi discharge coefficient
d	A diameter, ft
d _i	Inside diameter, ft
d _t	Venturi throat diameter, ft
E	Electromotive force, volts or millivolts
g	Gravitational constant, ft per sec ²
h	Heat transfer film coefficient, Btu per hr ft ² °F
I	Electric current, amperes
k	Thermal Conductivity, Btu per hr ft °F
k _a	Apparent thermal conductivity defined by Eq. III-5, Btu per hr ft °F
l	A length, ft
l _t	Length of test section, ft
m	A variable defined by Eq. 2, Appendix C
p	Pressure, consistent units
P	Electric power, watts
q	Heat transfer, Btu per hr
q ^l	Heat transfer per unit length, Btu per hr ft
Q	Volumetric flow rate, ft ³ per sec

r	A radius, ft
r_o	Outside tube radius, ft
R	Electric resistance, ohms
t	Temperature, °F
t_b	Bulk temperature, °F
t_f	Film temperature, °F
T	Temperature, °F
u	Velocity, ft per sec
y	Vertical distance between center of test section and center of heat exchanger, ft
α	Temperature coefficient of electrical resistivity, 1/°F
β	Temperature coefficient of thermal conductivity, 1/°F
β	Volume coefficient of expansion, 1/°F
γ	Specific weight, lb per ft ²
μ	Dynamic viscosity, lb sec per ft ²
ρ	Electrical resistivity, ohm ft
ω	Weight rate of flow, lb per hr

Dimensionless Groups

Gr	Grashof number, $d^3 \Delta t \beta \gamma^2 / \mu^2 g$
Nu	Nusselt number, $h d / k$
Pr	Prandtl number, $c_p \mu / k$
Re	Reynolds number, $\gamma u d / \mu g$

Subscripts

b	Bulk conditions
f	Film conditions
m	Mean conditions
t	Throat conditions

VITA

Eugene Charles Nestle

Candidate for the Degree of

Master of Science

Thesis: DESIGN AND CALIBRATION OF A THERMAL SYPHON HEAT TRANSFER
LOOP UTILIZING FREON 12 NEAR THE CRITICAL STATE

Major Field: Mechanical Engineering

Biographical:

Personal Data: Born in St. Louis, Missouri, August 6, 1934,
the son of Eugene M. and Marcella Nestle.

Education: Graduated from Holy Family High School, Tulsa, Okla.,
in May, 1952; entered Oklahoma State University in September,
1952, and received the Bachelor of Science Degree in Mechan-
ical Engineering in May, 1957; completed the requirements for
Master of Science Degree in August, 1958.

Experience: Worked in the steel tubing warehouse of the C. A.
Roberts Co., Tulsa, Okla., during the summers of 1954, and
1955; worked on the construction of burners and heating
equipment for the John Zink Co., during the summer of 1956;
served as a graduate teaching assistant while working on the
M. S. Degree at Oklahoma State University.

Professional Organizations: Member of the American Society of
Mechanical Engineers, Pi Tau Sigma, Sigma Tau, and is an
Engineer-in-Training (Oklahoma).